Reef-rim structure and building history, Rangiroa, an uplifted Atoll, French Polynesia: The role of morphotectonics and extreme marine hazard events

L.F. Montaggioni, Jean-Michel Baltassat, Gonéri Le Cozannet, Ch. Innocent, B. Martin-Garin, B. Salvat

Reef-rim structure and building history, Rangiroa an uplifted atoll, French Polynesia: the role of morphotectonics and extreme marine hazard events

L.F. Montaggioni [a,*], J.-M. Baltassat [b], G. Le Cozannet [b], Ch. Innocent, B. Martin-Garin [a], B. Salvat [c].

[a] Aix Marseille Univ, CNRS, IRD, INRAE, Coll France, CEREGE, 13331 Marseille, France

[b] Bureau de recherches géologiques et minières (BRGM) – Service géologique national, 45060 Orléans, France

[c] PSL-École pratique des hautes études, USR3278, EPHE, CNRS, UPVD, Labex Corail, CRIOBE, université de Perpignan, 66860 Perpignan, France

Corresponding author, Email address: montaggioni@cerege.fr

Highlights

- North of Rangiroa Atoll, due to a former uplift, the top of the Miocene carbonate basement peaks at depths of less than 10 m beneath the modern reef-rim surface.
- Unusual, extreme marine hazard events are likely to have contributed to ~~were essential drivers of~~ early atoll rim-island accretion.
- Island accretion started by about 6,000 calendar years, 3,500 years before it did in nearby subsiding atolls.

Abstract

Reconstructing the responses of low-lying, atoll-rim islands to future environmental changes due to global warming requires a robust knowledge of the building history of reef rims through time. In the northwest of Tuamotu Archipelago, atolls have experienced opposite vertical motions (uplift *versus* subsidence) in response to differential tectonic constraints undergone by the underlying oceanic crust. As a result, during Pleistocene high sea levels, some atolls remained emerged whereas others remained flooded. Based on two electrical resistivity tomography profiles across the northern rim-island of the uplifted Rangiroa Atoll and on U/Th dating of corals clasts collected from unconsolidated sand-rubble deposits within two wells through the same island area, the internal structure of the atoll-rim and its mode and timing of building are tentatively reconstructed. The irregularly shaped, upper boundary of the basal resistive unit is interpreted as residual, pinnacle-shaped reliefs of Miocene age. At the

seaward rim side, the uppermost highly resistive layers, an about 5 m-thick, were assumed to be reef-related, partly consolidated material emplaced during the Holocene. Thicker resistive layers that infill cavities in the Miocene basement, in the central part of the atoll rim, refer to the fresh water lense in porous, more or less consolidated material (phosphorites?) presumably emplaced during the Mio-Pliocene. In northern Rangiroa, the age of the oldest coral clasts trapped into the atoll-rim islands ranges between about 11,000 and 8,000 calendar years when sea level was approximately 60 to 20 m below its present position. This implies that coral-clast supply from the adjacent forereef slopes was triggered by extreme wave-surge events (presumably, tsunamis generated by island flank failures). The earliest island initiation phase is thought to start by approximately 6,000 cal. yr and to be achieved by about 3,000 cal. yr. By constrast, on the nearby subsiding Takapoto Atoll, the rim island began to initiate not earlier than 2,500 cal. yr. At Rangiroa, morphotectonics is assumed to have played a major role in controlling the internal rim architecture and, associated to extreme marine hazard events, to have promoted the earlier settlement of low-lying, rim islands through an earlier infilling of accommodation space as compared to nearby subsiding atolls.

Keywords

Atoll rim
Tectonics
Extreme hazard events
Rangiroa
Tuamotu
French Polynesia

Introduction

Sea-level rise and increasing storm intensity, due to ongoing climate change, are regarded as risking of opening high-water energy windows across low-lying island coasts, especially across tropical atolls (IPCC, 2019). The emergent, uppermost parts of atoll rims consist of low-lying coral-reef islands, usually composed prominently of loose coral rubble deposits in the form of small, continuous or scattered islets (*motu* in Polynesian language), usually less than 5–6 m in maximum elevation, mostly resting on firmly cemented, underlying conglomerate platforms (Biribo and Woodroffe, 2011; Montaggioni, 2011). Nowadays, atoll islands are receiving increased attention because the combination of sea-level rise and

extreme hazard events is likely to cause future irreversible damage to them, thus precluding any human occupation (Storlazzi et al., 2015, 2018). Recent observations indicated ~~showed~~ that atoll islands are experiencing various evolutionary patterns, including stability, erosion and accretion (Kench et al., 2018; Duvat et al., 2020). This suggests that, over the next centuries to millennia, atoll islands should respond differentially to the future sea-level rise, projected to elevations of metres (Clark et al., 2016; IPCC, 2019).

Reconstructing detailed histories of atoll-rim building is a prerequisite to better understand atoll-island behaviours when faced with environmental changes at a millennial scale (East et al., 2018; Montaggioni et al., 2018, 2019a). Previous studies in a number of reef sites in the Indo-Pacific province revealed that rim-island development has started not before 5,000–4,800 cal. yr and continued until 2,800-2,500 cal. yr in both the Western Indian Ocean (Maldives: Kench et al., 2005; East et al., 2018) and the western and central Pacific – northern Great Barrier Reef of Australia: Kench et al., 2012; Marshall Islands: Kench et al., 2014. Low-lying, rim-island development has been interpreted as resulting from the interplay between reef growth and the rate of sea-level changes over the last few thousands years (Pirazzoli and Montaggioni, 1986; Richmond, 1992; Dickinson, 1999; Woodroffe et al., 1999; Kench et al., 2005; Woodroffe, 2005; Barry et al., 2007; Kench et al., 2014 a, b; Perry et al., 2011; East et al., 2018; Montaggioni et al., 2018, 2019a). Low-lying reef islands have been capable of accreting under various eustatic regimes. Their development has occurred either during a rise in sea level and sea-stands higher than the present (McLean et al., 1978; Stoddart et al., 1978; Woodroffe and Morrisson, 2001; Kench et al., 2014a,b; Yamano et al., 2014; East et al., 2018) or later, during a post-highstand sea-level fall (Woodroffe et al., 1999; Dickinson, 2009; Kench et al., 2014 a,b: Yasukochi et al., 2014; Montaggioni et al., 2018, 2019a).

In northwest Tuamotu (French Polynesia, central south Pacific), apart from subsiding atolls (Takapoto, Takaroa, Ahe, Manihi), there are also several uplifted atolls. These form a continuous belt composed of Makatea, Mataiva, Tikehau, Rangiroa, Kaukura, typified by exposed, partly dolomitized limestones of Miocene age (Delesalle, 1985; Harmelin-Vivien, 1985; Montaggioni, 1985; Ricard, 1985). This island belt is facing the northwest sides of Tahiti and Moorea Islands in the Society Archipelago. Uplifting was thought to have been caused either by a lithospheric flexure in response to volcanic loading generated by nearby Tahiti-Moorea volcanoes (McNutt and Menard, 1978; Lambeck, 1981) or by an underlying asthenospheric bump in relation to the Society hotspot swell (Menard, 1973; Crough, 1983) during the early Pleistocene (Montaggioni, 1989; Montaggioni and Camoin, 1997). As a

consequence, even during most episodes of mid Pleistocene to Holocene high sea stands, these atolls occurred as high rising reliefs. At those times, coral communities have grown in the form of apron reefs plastered against their submarine flanks, as currently observed on the nearby high carbonate Makatea Island (Montaggioni, 1985; Montaggioni and Camoin, 1997). This accounts for the absence of exposed Pleistocene reef units capping the atoll rims. Only, a few meter-thick mid to late Holocene reef deposits are overlying the Mio-early Pleistocene rim surfaces (Rougerie et al., 1997). By contrast, as shown on the nearby subsiding Takapoto Atoll, during the mid to late high sea stands Pleistocene, the top reef surfaces stage (Montaggioni et al., 2019b) were regularly submerged, thus resulting in the overlaying of a number of successive reef generations (Montaggioni et al., 2019b).

While sea level reached its present position by about 6,000 years BP, on Takapoto, the Holocene reef unit in the making reached the position of present sea level not prior to 3,000 cal. yr. The initiation of modern, low-lying rim-islands started approximately 2,500 years ago, as sea level was about 0.60–0.30 m above present sea level (Montaggioni, 2018, 2019a).

Using Rangiroa as a representative test area for uplifted atolls, the objectives of the present study are to: (1) reconstruct the internal structure of the upper parts of the uplifted atoll-rim pile, based on electrical resistivity tomography; (2) to test the hypothesis that, during the Holocene, these atoll-rim surfaces have served as substrates for earlier initiation and emplacement of low-lying rim islands as compared to subsiding atolls in the northern Tuamotu. The neighbouring Takapoto Atoll will be used as a dipstick of subsiding atolls; (3) demonstrate that morphotectonics and extreme marine hazard events in the considered region have played a major role in atoll-rim development in addition to changes in accommodation space.

Environmental setting

Rangiroa Atoll is located in the northwestern part of the Tuamotu Archipelago, between latitude 14°59'–15°19' south and longitude 148°00'–147°10' west, approximately 200 km northeast of Tahiti (Fig. 1A). Reaching 7 m in maximum elevation (Duvat et al., 2020), the atoll is 80 km long, aligned along a WNW–ESE main axis, and 33 km in its widest part. The total atoll area is about 1,000 km^2. The lagoon is 35 m to 55 m deep in its deepest parts. The reef rim is larger in the northern sector (750–1100 m) than in the western and southern ones (300–600 m). About 30 % of the total atoll-rim surfaces are occupied by islands, composed of a series of gravelly to sandy islets (Fig. 1B), locally resting on a subhorizontal, cemented

conglomerate platforms, less than 1m-thick on average. The outer parts of the atoll rim consists of a reef-flat zone ranging from 50 to 200 m in width and is locally bounded seawards by a raised outer edge with a well-developed (10–20 m wide) algal ridge (Stoddart, 1969). Scuba diving surveys off Avatoru village (B. Martin-Garin, pers. observ.) revealed that the upper forereef zone consists of a spur-and-groove system, extending over 100 m oceanwards, from sea surface to about 8–9 m below pmsl. This system ends on an upper, gently dipping terrace, up to 50 m wide, ranging between 9 m and 11 m in depth. This terrace is followed downslope by a drop-off extending to a depth of 60 m. A lower terrace, about 50 m in maximum width, develops between 60 m and 62 m deep and ends on a subvertical wall falling to depths greater than 100 m (Fig. 2).

The reef-flat surfaces are colonized by small *Porites* and *Acropora* colonies, not exceeding 10 % in cover rate (Ricard, 1985). Long-term coral monitoring from a selected forereef area, i.e. the upper terrace, at 10.5–11 m deep off Avatoru village – 14°56'46'' south; 147°41'62'' west – indicated that the total coral cover rate has varied between 31 % and 52 % from year to year over the last two decades. The dominant coral forms are branching *Pocillopora* (22 to 27 %) and massive *Porites* (9 to 12 %), together with *Montipora* (0 to 14 %) and *Acropora* (0 to 6 %) – data courtesy by Service d'observation national CORAIL, CRIOBE, Moorea Island, French Polynesia.

Along the southern outer reef rim, are found deeply pitted and dolomitized, pinnacle-shaped limestones, up to 3 m in height (Fig. 3). These pinnacles, referred to as *feo* by Polynesians, were interpreted as remnants of formerly uplifted reef-related frameworks of late Neogene to Pleistocene age (Vahrenkamp and Ginsburg in Ricard, 1985), demonstrated to be of late Miocene age from paleontological records (Montaggioni, 1989; Montaggioni and Camoin 1997).

As for the other northwestern Tuamotu atolls, Rangiroa is influenced by the southeast trade-winds, blowing from the ENE sectors for 70 % of the year and for 20 % from the SE sector. In the austral winter (May to October), 2.5-m high swells with long periods (> 10 s) are generated by strong trade winds. During the austral summer (November to April), trade winds are less active and generate a moderate hydrodynamic regime, locally determined by storm events initiated by ENSO-related cyclones or by storms originating from northern latitudes (Andréfoüet et al., 2012). Cyclones come usually from the northeastern and northwestern sectors, with a frequency of one to three events per century (Dupon, 1987; Gabrié and Salvat, 1985; Larrue and Chiron, 2010). The rim islands suffer occasional damage due to cyclone activity. For instance, the 1983 cyclonic events have resulted in significant

shore disturbance and reshaping, including strong reworking of sandy beaches and deposition of new shingle ridges along the northern and western, ocean-facing shorelines (Ricard, 1985). Tides are a twice-daily regime and microtidal, averaging 0.20 m in amplitude and reaching a maximum of 0.50 m at spring tide. In northern Rangiroa, historical tsunamis are known to have usually generated only low-frequency and low-amplitude (1–2 m-high) swells (Sladen et al. 2007).

Materials and methods

Electrical resistivity tomography (ERT)

ERT is a geophysical imaging technique, based on measurements of electrical resistivity in subsurface rocks (Schroot and Sass, 2008) using direct current. In reef systems, in absence of clay, resistivity depends on limestone lithology, more specifically, on the degrees of cementation and porosity, on water content and salinity (Comte et al., 2010; Join et al., 2011). Resistivity therefore is a reliable tool used to discriminate: i) high resistivity, cemented limestones from low resistivity, porous and aquifer limestones; ii) low resistivity, saline intrusions from medium resistivity, fresh water lenses. Nevertheless, lithological and fluid effects may interfere, thus leading to undetermination (Schrott and Sass, 2008; Youssef et al., 2012; Carrière et al., 2013). In the northern part of Rangiroa atoll-rim, close to Avatoru village, ERT was used to characterize subsurface rock heterogeneities and the salt-water/fresh-water interface geometry.

Two 2D cross-island profiles oriented perpendicular to the shoreline were surveyed using a multi-electrode system in dipole-dipole (DD) and Wenner-Schlumberger (WSR) array configuration (Fig. 1C). The electrode arrays were spaced 10 m apart for lengths of 790 m (P1) and 860 m (P3) respectively. The reached maximum investigation depth was about 150 m. These profiles have followed gentle island topography from the ocean-facing shoreline to the lagoon border. The electrodes were hammered into the loose soil and surficial island deposits and seawater was used to enhance electrode contact resistances, all of which were checked to be of same order between a 0.5 $\Omega \cdot$ m to 3.0 KΩ. A Syscal Pro® resistivity-meter with multinodes, system of 250 W power from Iris Instrument was applied to collect the resistivity data. With 96–99 % (WSR) to 85–94 % (DD) data usable after screening, the data are considered to be of good quality. Measured resistivity were inverted using Res2Dinv® software from Geotomography using the blocky option (Loke et al., 2003). This

option lies on mean square regularization minimizing the sum of the absolute values of the data misfit. It is applied to the model roughness filter, resulting in a better accommodation of high resistivity contrasts and data outliers and tending to produce models consisting of areas with piecewise constant resistivity (Farquharson and Oldenburg, 1998; Loke et al., 2003) with a better resolution of discontinuities (Seaton and Burbey, 2003).

Inversion of surface tomography data is an illposed problem and different resistivity model obtained as a result of inversion may satisfy the same dataset with a given RMS misfit. The presented resistivity images are one solution among many possible solutions; but using the blocky option applied to the combined DD and WSR dataset, these images present a reliable determination of underground geometry. With the 10-m electrode spacings, modeled cells are typically representative of plurimetric-wide heterogeneities at shallow and mid depths to up to tens of metres deeper.

Coral sampling and radiometric dating procedures

Coral samples were collected from two water wells dug through the northern parts of the island (Fig. 1C). Well 1 is located close to Avatoru village, at a distance of about 200 m behind the outer coastline. Well 2 is located on Vaineate site at a distance of about 300 m from the coastline, backward the runway. The well entrances (island surface) are at elevations ranging from 2–2.3 m (Well 1) to 1.5–1.6 m (Well 2) above present sea level (pmsl) (Fig. 4). Sampling was carried out randomly along the internal walls. These consist of a mixture of skeletal sands and gravels, with some coral cobbles and pebbles (Fig. 5). In Well 1, samples were taken at depths of 1.5 m (Sample Rangiroa 1-1) and 2 m (Sample Rangiroa 1-2) respectively beneath the island surface along the southern and northeastern wall sections. The bottom of the well is occupied by an indurated conglomerate platform, about 0.30 m high above pmsl. In Well 2, Samples Rangiroa 2-1 and 2-2 were taken respectively at depths of 1.5 m and 1 m beneath the island surface along two opposite wall sections. The bottom of Well 2 is made up of loosely consolidated gravelly-sand material (Fig. 5). As a supplement, given that surficial deposits at the vicinity of the wells were reworked during excavation works, a third sample (Sample Rangiroa Défense) was extracted from the top surface of an old quarry located close to the city hall of Avatoru, in order to estimate the average age of deposition of the uppermost layers in the considered rim islet. As demonstrated in a number of previous studies (see Montaggioni et al., 2018, 2019a and references herein), radiometric dating of coral clasts from atoll rim excavations and drillholes can be used to attempt

reconstructing the mode and timing of reef islet accretion.

Uranium-thorium dating was carried out on coral samples. They were gently crushed and the cleanest parts were selected for analysis. A few hundreds of milligrams were dissolved in dilute HCl. U and Th analyses were done after chemical separation at BRGM (Orléans, France) on a Neptune MC-ICPMS mass spectrometer. Details on chemical separation and mass spectrometry can be found in Innocent et al. (2005) and Millot et al. (2011). Results are reported in Table 1.

All but one samples display uranium contents close to 3 µg/g (Fig. 6A), which is known to constitute the average value of living corals (Edwards et al., 1987). Thus, this strongly suggests that the samples with lower uranium contents were not affected by any early cementation or secondary recrystallization, despite their early to mid Holocene ages. Only the Rangiroa Défense sample displays higher U contents (Table 1, Fig. 6B).

Thorium concentrations are very low, ranging from < 1 ng/g to 28 ng/g for Sample 1-1 (Table 1). Sample Rangiroa 1-1 and, to a lesser extent, Sample Rangiroa 2-1 emphasize the occurrence of minute amounts of detrital Th. Uranium activity ratios are similar to the present-day seawater value within uncertainty (Chen et al., 1986) (Table 1, Fig. 6B).

Ages have been calculated from $^{230}Th/^{234}U$ ratios. As corals are of young age, the effect of the decay of excess ^{234}U can be neglected. Conversely, calculated ages should be corrected for the initial ^{230}Th of detrital origin. Calculations have been done with a $^{230}Th/^{232}Th$ activity ratio of 0.78, corresponding to a ^{238}U decay chain at secular equilibrium, and to an elemental Th/U ratio of 4, typical of the value of the average outcropping continental crust. The correction effet remains very slight.

Ages are expressed in calendar years relative to the year of sample analysis (2018) during which uranium-thorium dating were conducted.

Results and discussion

Resistivity imaging the internal structure of the upper parts of the atoll-rim pile

Geophysical results are interpreted in terms of types of depositional environments through *resistivity units*, i.e. relatively resistive (Rn) or conductive (Cn). These units are defined as areas of uniform resistivity, showing a high gradient of resistivity towards neighbouring units. The limits between resistivity units refer to as *discontinuities* and are defined at the maximum

gradient of resistivity between areas of uniform resistivity. These resistivity units can relate to varying geological features, including sedimentary layers, lenses, rocky blocks of varying lithological and mineralogical composition, or varying hydrological features (aquifers, fresh water lenses, salted intrusion) affecting a same carbonate formation. Accordingly, limits between the resistivity units may be those delineating different geological features, between bodies of different lithology within a same formation or those indicative of tectonic features such as faults, fractures or unconformity surfaces and fresh/saline water interface as well.

Different interpretations can be proposed for a same resistivity unit. It is also possible that some geological features, due to their limited thickness and extension and/or limited or no resistivity contrast, cannot be detected and imaged by ERT and, as such, are not expressed in resistivity images. The various resistivity units as defined in P1 and P3 tomographies are presented in Table 2 and Figures 7A and 7B. Resistivity variations are presented as color-countered images of subsurface resistivity variations. For the two profiles, high resistivity–low conductivity zones were delineated by purple-red while low resistivity–high conductivity zones by blue-green. Transitional conditions were identified by yellow to brown colors.

The two 2D cross-island electrical resistivity profiles (P1, P3) image the internal structure of the upper parts of the atoll-rim pile to maximum depths of about 150 m (Fig. 7A, 7B). The inversion-derived resistivity models show significant variations in resistivity from the ocean side to the lagoon, especially near and beneath the atoll-rim surface. At depth, there is a resistive basement R3 (90–240 $\Omega \cdot$ m) at the seaward side. R3 has more upward resistive columnar extensions (R3', R3'' with $240 < p < 700$ $\Omega \cdot$ m) in irregular, indented contact with the overlying conductive layers C3 and C3'. At the same rim side, resistivity unit R4 ranges from about 90 $\Omega \cdot$ m to up to 700 $\Omega \cdot$ m over a 200 m (P1) or a 450 m (P3) distances inwards, close to the island surface (Fig. 7A, B). Red to brown-coloured R4 forms 5-10 m-thick, horizontal, plate-shaped structures. In P1, between surface to depths of about 30 m, shallow (R2) and less shallow (R1) resistive units ($100 < p < 250$ $\Omega \cdot$ m) are covering the central, upper part of the atoll-rim pile. Lagoonwards, resistivity are markedly lower, varying from about 100 to less than 1 $\Omega \cdot$ m from the surface to several tens of meters. The very conductive, blue cover C4 ($0.3 < p < 5$ $\Omega \cdot$ m) extends more deeply beneath the atoll surface, through more (C4'') or less conductive (C4') dark green intrusion, over an even less conductive, light green basement C5 ($20 < p < 60$ $\Omega \cdot$ m) (Fig. 7A, B).

Geological and hydrological interpretation of resistivity imagery

The geological interpretation of the overall resistivity variations (Table 2, Fig. 7C) is mainly qualitative and based on field observations and partial knowledge of the development history of Rangiroa and nearby atolls (see Delesalle, 1985; Montaggioni, 1985, 1989; Ricard, 1985; Montaggioni and Camoin, 1997; Montaggioni et al., 2019a,b)

The uppermost, most resistive bed (R4), averaging 5-6 m-thick and extending over about 450 m from the shoreline landwards is interpreted as related to Holocene deposits (Fig. 7C). In the absence of local drilling investigations, the nature of R4 could be identified by analogy with deposits penetrated through rim-island areas from the nearby atolls of Mataiva and Tikehau, given the latter have proven to follow a geological evolution similar to that of Rangiroa (Delesalle, 1985; Harmelin-Vivien, 1985; Ricard, 1985). Reef drilling in both atolls revealed that the limestone basement is directly covered by unconsolidated to partly consolidated rubble-sand material of postglacial to Holocene age. Local induration is presumably due to the fact that the lower parts of the Holocene deposits are standing below the water table, in the phreatic zone, thus favoring intergranular cementation. On Mataiva, Holocene deposits are 4 to 6 m-thick at rim-island sites (Delesalle, 1985; Pirazzoli and Montaggioni, 1986). On Tikehau, the atoll rim is covered with Holocene detritus, less than 5 m-thick (Rougerie et al., 1997). Accordingly, in northern Rangiroa, at the studied rim sites, an expected 5 to 6-m thickness of Holocene sediments is in good agreement with those from the two neighbouring atolls. It is noteworthy that, on these three atolls, there is no evidence of exposed or buried Pleistocene highstand reef units beneath the Holocene deposits.

In addition, at Rangiroa, along the studied seaward face, there are isolated R4 elements with highest resistivity that may be regarded as isolated, cemented megaclasts trapped into the Holocene deposits. Numerous megaclasts, i.e. pieces of spurs extracted from the uppermost forereef zone, about 10-15 m^3 on average, are exposed on the reef-flat zone, at the northern end of the atoll (Ricard, 1985) and some of them are likely to be buried locally. Less resistive, scattered features (R1, R2) are found centered beneath the middle part of the atoll rim from the subsurface to depths of 30 m. These could be reworked remains of the limestone basement found deeper (Fig. 7C). Indeed, more internally, between approximately 10 m and deeper than 120 m, there are high cohesive, pinnacle-shaped structures (R3), regarded as residual, firmly indurated limestone reliefs (Fig. 7C). These reliefs are similar to *feo* restricted along the southern, outer rim (Fig. 3) and to those found in the neighbouring atolls of Mataiva, Tikehau

and Kaukura. In a lack of conclusive dating, an early Miocene age for these feo is most likely by analogy with similar biostratigraphically dated rock occurrences on the nearby high carbonate island of Makatea (Montaggioni, 1985; Montaggioni et al., 1985; Montaggioni, 1989; Montaggioni and Camoin, 1997). Differences in elevation of about 20-30 m between the remnants of dolomitized limestones present in the south and their expected, subsurface counterparts in the north are thought to be due to a more severe karstic alteration in the northern parts of the carbonate pile during successive periods of emergence. The strict location of *feo* along the southern, outer reef-flat zones cannot be explained as resulting of a northward tilting of the atoll and a subsequent differential uplift, since, on nearby uplifted atolls (Mataiva, Tikehau, Kaukura), *feo* are distributed randomly from south to north. Differential sub-aerial erosion between south and north of Rangiroa may have been generated locally by fracture networks, known to develop parallel to some reef-front lines on the northern Tuamotu atolls (Chevalier et al., 1968, Faure and Laboute, 1986; Montaggioni et al., 2019b).

The conductive C1, C3 anomalies mostly located above R3 structures might refer to porous, poorly consolidated deposits. These are infilling karstic cavities within the Miocene limestones (Fig. 7C). On nearby Makatea and Mataiva Atolls, karst cavities are known to be infilled by sand-grained phosphatic material (Obellianne, 1963; Montaggioni, 1985; Trichet and Fikri, 1997) regarded to be Mio-Pliocene (Montaggioni, 1989; Montaggioni and Camoin, 1997) rather than mid Pleistocene (Aharon and Veeh, 1984). Similar sandy phosphorites might be present directly beneath the Holocene unit at Rangiroa. Shallow to deep, more or less conductive features (C4, C4', C4") southwards close to or at lagoon sites, probably result from dense saline intrusion in more or less permeable deposits (Fig. 7A, B). These deposits may be phosphates, at least in part, covered by Holocene material (Fig. 7C).

Validity of U/Th dating from removed coral material

The value of U/Th measurements from removed skeletal material used as proxies for defining the timing of building of low-lying, atoll-rim islands has been previously debated thoroughly by Woodroffe et al. (1999, 2007), Kench et al. (2014a, b), and Montaggioni et al. (2018, 2019a). It has been suggested that time intervals separating the time of death of a given organism from the time of deposition and final stabilisation of the relevant skeleton could range from tens to hundreds of years as clearly evidenced by age inversions in the stratigraphic sections. Consequently, reconstruction of island chronology should be

349 considered as relative rather than absolute. The coral-clast samples with mean ages relative to
350 all dated samples can serve to estimate the mean date in terms of deposition. By contrast, the
351 ages of youngest samples usually found close to the upper parts of wells produce estimates of
352 the time at which the main vertical island accretion phase has ended.

353 **Chronology of rim-island accretion**

354 U/Th dating of the pebble-sized coral clasts from the well sections excavated through the
355 northern part of Rangiroa provides ages ranging between 11,546 ± 131 and 3,098 ± 57 yr BP
356 (Table 1, Fig. 5). This means that the oldest coral clasts were moved from the adjacent
357 foreslopes along which coral populations were growing and projected onto the upper atoll-rim
358 surfaces while Rangiroa was an emergent carbonate island, initially at about 35–40 m high.
359 Taking into account possible storage and reworking of clasts before incorporation into rim-
360 island deposits and based on their mean ages, rim-island development is expected to have
361 started by approximately 6,000 cal. yr. At that time, sea level was close to its present position
362 (Figs. 8, 10).

363 **The role of morphotectonics in the contrasting atoll-island building histories**

364 As the other nearby uplifted atolls, Rangiroa is considered to have experienced uplifting,
365 probably at the beginning of the Quaternary (Montaggioni, 1989; Montaggioni and Camoin,
366 1997). Uplift has resulted at present in the emergence of remnants of the Miocene limestones
367 in its southern part or located at depths of less than 10 m below the modern rim surface in its
368 northern part. Otherwise, there is no evidence of exposed last interglacial reefs at Rangiroa
369 while this reef generation is assumed to have developed between +9 to +6 m above present
370 sea level between 128 to 116 ka (Kopp et al., 2009; Dutton and Lambeck, 2012; Murray-
371 Wallace and Woodroffe, 2014). This indicates that the relevant reefs are currently submerged,
372 which means that the uplifting effects have ended at least since the last interglacial times and
373 Rangiroa is now subsiding. This may be due to the fact that the lithospheric bulge generated
374 by the loading of Tahiti and Moorea volcanoes is experiencing an active deflation or Rangiroa
375 is at present situated at a distance long enough to escape the bumping effects of the Society
376 hotspot swell. Consequently, thermal subsidence of the underlying oceanic crust has taken up
377 its course as it did prior to the uplifting event, according to the standard cooling plate model
378 (Parsons and Sclater, 1977; McNutt and Menard, 1978; Marty and Cazenave, 1989). Despite
379 relatively recent subsidence resumption, the Miocene pile appears to have acted as a shoal-

water or emergent morphosystem throughout the Pleistocene to Holocene, thus usually leading to coral growth in the form of apron to fringing reefs along the submarine flanks of the atoll. By contrast, the atolls further to the northeast, including Takapoto, have been continuously subsiding since the cessation of volcanic activity (Talandier and Okal, 1987), likely to the Eocene times (Ito et al., 1995), thus permitting the vertical stacking of successive Pleistocene high-stand reefs over the atoll rim (Montaggioni et al., 2019b).

The contrasting geodynamical history of Rangiroa and Takapoto Atolls would partly explain the contrasting development history of their respective rim islands. In northern Rangiroa, despite the limited number of dated samples, the provided ages clearly indicate that rim-island accretion may have started not later than 6,000 cal. yr, according to the mean ages of the dated samples. Assuming a mean vertical reef accretion rate of 4-5 mm/yr over the mid Holocene (Dullo, 2005; Montaggioni, 2005), the accommodation space created by the postglacial rising sea level was totally infilled by 6,000 cal. yr, at the time when sea level reached its present position. This resulted in the formation of reef-flat surfaces at sea level. These surfaces have served as depocenters for island initiation. The main accretional phase is likely to have occurred between 6,000 and about 3,000 cal. yr (Figs. 8, 10).

At Takapoto, a dataset of 80 radiometrically dated coral samples were obtained from 8 excavations dug through the windward, southeast and leeward, southwest part of the island (Montaggioni et al., 2018, 2019a). Except for one basal sample dated 7,705 ± 120 cal. yr, the remaining 79 samples (98.75 % of total sampling) yielded ages not exceeding 2,958 ± 17 cal. yr (Fig. 9). This means that the emplacement of the island deposits at Takapoto occurred during the late Holocene, at a time of relative sea-level fall in the region (Pirazzoli and Montaggioni, 1988; Rashid et al., 2014; Halmann et al., 2018, 2020). From 8,000 to 6,000 cal. yr, contrary to Rangiroa, the rim at Takapoto was submerged at depths of about 5-6 m relative to present, thus delaying the initation of island building (Fig. 11).

The role of unusual marine hazard events in the timing of rim-island building at Rangiroa

Coral detritus is likely to have derived from the adjacent foreslopes as observed in nearby atolls (Hamelin-Vivien and Laboute, 1986; Montaggioni et al., 2018). Extraction of living coral colonies from outer reef slopes and subsequent projection onto emergent rim surfaces are known to be common processes triggered by severe cyclone hits (Harmelin-Vivien and Laboute, 1986; Harmelin-Vivien, 1994). In addition, as mentioned above, reef megaclasts

(*cyclopean blocks*) are found in great number on Rangiroa, resting on the reef-flat zone, especially along the northern area, most exposed to cyclones (Stoddart, 1969; Bourrouilh-Le Jan and Talandier, 1985; Ricard, 1985). Similarly, several atolls within the French Polynesian realm exhibit similar features (Etienne, 2012; Toomey et al., 2013; Lau et al., 2016). Given the scarcity and low magnitude of tsunami events hitting coasts in the Tuamotu, the motion of reef megaclasts was usually interpreted as triggered by high intensity cyclones (Canavesio, 2014; Canavesio et al., 2018). However, the most striking feature at Rangiroa is that pebble-sized coral clasts dated at about 11,500 to 8,700 cal. yr have been extracted from the adjacent forereef slope when sea level was between 55 and 40 m below present.

Two alternative scenarios could be invoked for explaining the incorporation of early Holocene coral fragments into atoll-island deposits: step-by-step transport with transient deposition on terraces located at mid-depth prior to be removed upwards; single-stroke transport upwards and deposition along the margins of the atoll-rim tops prior to be removed inwards. Along the forereef slopes in front of Avatoru village, there are two terraces, respectively at depths of 8–11 m and 60–62 m. Assuming that the upper terrace has served as a transient depositional zone for coral detritus of early Holocene age prior to be deposited at the atoll-rim top, the relevant coral colonies have necessarily jumped approximately 45 to 30 m from their life space. These coral detritus are expected to have been stored on the outer borders of the atoll rim and occasionally displaced inwards to contribute to the accretion of basal conglomerates and island deposits.

Cyclone-generated surge impacts on foreslopes demonstrated to be efficient at depths not exceeding 20 m. From these depths, broken colonies can be displaced upslope to atoll-top surfaces (Harmelin-Vivien and Laboute, 1986; Harmelin-Vivien, 1994). Consequently, whatever the scenario invoked, cyclones cannot have been originally involved in the extraction of the oldest coral colonies at present trapped into the studied island sites. The most likely explanation is that the moving force able to transport coral clasts at unusual elevations were paroxysmal wave surges, maybe generated by occasional tsunamis known to be of very low-frequency when compared to cyclones (Lau et al., 2016).

Similar hazard events have been described in a number of other tropical locations. Coral clasts, ranging in size from pebbles to blocks, deposited at unusual heights (10–40 m), not related to high sea stands, were found occasionally along tropical volcanic coasts, as on Mauritius and Rodrigues Islands, Western Indian Ocean (Montaggioni, 1978). Their uncalibrated radiocarbon ages range from around 6,000 to 3,700 yr BP. Especially, an isolated, overturned, massive *Porites* head, about 2 m^3 in volume, was encountered at the

446 elevation of 40 m above pmsl at Gunner's Quoin Island, 8 km north of Mauritius. Its age is
447 5,730 ± 120 uncalibrated yr BP (Montaggioni, 1978). At that time, sea level was about 5–6 m
448 below pmsl (Camoin et al., 2001). This indicates that the removed *Porites* colonies has
449 experienced a 45 m-high jump at least, prior to be deposited. Similarly, Paris et al. (2013)
450 mentioned a 0.20–0.45 m-thick, mixed pebble- to block-sized coral-volcaniclastic
451 conglomerates, 4,425 ± 35 calibrated yr BP old at 10–15 m above pmsl on the southern coast
452 of Mauritius. Although it could be deemed inappropriate to compare the transport and
453 deposition conditions of pebble- and megablock-sized material, throwing of differently sized
454 clasts from coral communities living at several tens of meters is likely to require extreme
455 wave heights, irrespective of hydrodynamical processes invoked. As demonstrated from
456 several volcanic islands, including the Society, although there would have no statistic
457 correlation between sea-level rise and volcano flank collapses, 25–30 % of the identified
458 submarine landslides were demonstrated to have been coeval of rapid (> 5 mm/yr) sea-level
459 rise (Paris et al., 2013). Flank collapse records from Cape Verde Islands (Atlantic Ocean)
460 revealed that landslide-generated tsunamis may occur at a frequency of one to three every ten
461 thousands years (Paris et al., 2013).
462 Several flank collapse events have been identified from high volcanic islands in French
463 Polynesia as from Tahiti and Austral Islands (Clouard and Bonneville, 2003, 2004; Clouard et
464 al., 2001) and from Tuamotu atolls as Takapoto (Montaggioni et al., 2019b). Such processes
465 might easily explain displacement of coral gravels and pebbles to unusual altitudes as
466 observed in northern Rangiroa.

467 **Comparative models of low-lying, rim island development**

468 In French Polynesia, from 12,000 cal. yr, sea level rose from a depth of about 60 m relative to
469 present, at a mean rate of 10 mm/yr (Bard et al., 1996). It reached and overpassed its present
470 position by 6,000 cal. yr (Pirazzoli and Montaggioni, 1988; Bard et al., 1996, 2010; Hallmann
471 et al., 2018, 2020) (Fig. 8). On the basis of the electrical resistivity tomography profiles from
472 northern Rangiroa and by analogy with the nearby uplifted Mataiva and Tikehau Atolls, the
473 upper, partly indurated atoll-rim units, about 5 m-thick, were tentatively attributed to the reef
474 unit emplaced during the course of the rising sea level. On the subsiding northwest Tuamotu
475 atolls, including Takapoto, according to the mean vertical coral-reef accretion rate (4–
476 5 mm/yr) estimated for early to mid Holocene (e.g. Dullo, 2005; Montaggioni, 2005; Hubbard
477 and Dullo, 2016; Perry et al., 2018; Gischler and Hudson, 2019), the rate of the rising sea

level is most likely to have been too rapid to allow coral growth maintaining pace with sea level. This resulted in the opening of a wider accommodation space. Indeed, the MIS 5e reef tract, that is expected to underlie the modern atoll-rim (Montaggioni et al., 2019b), would have been submerged under about 10 m of water by 7,000 cal.yr..

Unlike Takapoto, since the mid Holocene, most areas of the Rangiroa atoll–rim remained emerged or close to sea surface, as indicated by the occurrence of emergent, up to 3 m-high *feo* in the south (Fig. 3) and by electrical resistivity profiles showing similar geomorphic features beneath the atoll-rim surface in the north-east (Fig. 7). In northern Rangiroa, when sea level was approximately 50 to 30 m below pmsl, coral detritus have been extracted from adjacent forereef slopes. The oldest extracted coral clasts were dated from the early Holocene (Samples Rangiroa 1.1 and 2.1: 11,546 ± 131 and 8,769 ± 205 cal. yr, respectively). During the 11,000–9,000 cal. yr interval, the atoll-rim top was situated at elevations changing from about 40–45 to 30–35 m. In spite of its high rise, Rangiroa, at least in the northeast, is believed to have been clast-supplied by exceptionally high-amplitude, tsunami-generated surges. Coral clasts may have been originally trapped along the outer borders of the exposed atoll rim. By 8,000 cal. yr, the atoll-rim surfaces culminated at about 15 m above sea level (Fig. 10A). Based on the mean ages of coral clasts found in wells (Table 1), clast deposition is thought to have given rise to incipient depocenters by about 6,000 cal. yr (Fig. 10B) as sea level reached its present position. At that time, older coral clasts were removed occasionally inland to participate in island building. The main phase of island building was achieved presumably by about 3,000 cal. yr, as suggested by the age of the youngest coral speciment (Sample Rangiroa Défense: 3,098 ± 57 cal. yr) during a relative sea-level drop (Fig. 10C).

The neighbouring subsiding atolls, such as Takapoto, were emerged at elevations of around 9-10 m above pmsl, respectively by 8,000 cal.yr (Fig. 11A). The emergence episode resulted in deposition of the coral sample dated at 7,705 ± 120 cal. yr, found at the lowermost part of the southeast, island sequence (Montaggioni, et al., 2018). At that time, the atoll-rim top was capped with a MIS 5e reef unit (Montaggioni et al., 2019b). Later, this reef terrace was recolonized by coral populations and as such, was regularly depth-decreasing in response to infilling accommodation space by early to mid Holocene coral growth (Fig. 11B). Island initiation appears to have started only after the final emplacement of the modern reef flats, not before 2,500 cal. yr. Islands have continued accreting until about 1,500 cal. yr at a time when sea level was falling down to its present position (Figs. 8, 11C).

Over the last 3,000 years in north Rangiroa and over the last 1,500 years at Takapoto (Montaggioni et al., 2019a), rim islands are likely to have continuously extended from the initial depocentres seawards and lagoonwards owing to cyclone activity, resulting in the present-day island physiography (Fig. 12).

Conclusions

Reconstruction of the internal atoll-rim structure and recent building history of rim islands in the northern areas of the uplifted Rangiroa Atoll permits to gain the following new findings:

1– The uppermost, a few metres-thick, high resistive anomalies within the rim pile were assumed to be Holocene reef-related deposits, composed of partly consolidated rubble and sands, probably trapping isolated megaclasts. The other, irregularly shaped, high resistive anomalies found at depth were thought to be dolomitized remnants of the Miocene carbonate pile. The lower resistive material, which infills cavities within the pile, is interpreted as unconsolidated, sandy, porous phosphates, presumably Pliocene in age.

2– Coral-clast supply resulting in rim-island initiation started at a time when Rangiroa was raised at elevations of several ten meters above sea level. Only paroxysmal hazard events, such as tsunamis generated by island flank collapses, may explain clast deposition at unusually high elevations.

3– Differential vertical motions – uplift followed by subsidence resumption versus continuous subsidence – have given rise to different insular morphosystems in the northwest Tuamotu Archipelago. These have contributed to drive the timing and mode of rim-island buiding through controlling the width of opened accommodation spaces. During the early Holocene, accommodation space was about 5 m-wide at Rangiroa and 10 m-wide at Takapoto. Accordingly, island initiation in northern Rangiroa appears to have happened out of phase with that in nearby subsiding atolls as Takapoto. The combination of long-term emergence due to uplift and of unusual surge regime has resulted in a markedly earlier island settlement as soon as the early Holocene. Earliest supply of coral detritus to the rim top surfaces seems to have started prior to 11,000 cal. yr, at least 4,000 years earlier than at Takapoto. The main episode of island development is likely to have occurred during episodes of rising sea level, from about 6,000 to 3,000 cal. yr.

Acknowledgements

Field work at Rangiroa has benefited from financial support of the BRGM (Bureau de recherches géologiques et minières, Orléans, France) in the frame of INSeaPTION Project (Grant 690462). We thank Lyona for allowing and facilitating acces the wells, Esther Mercier (Creocean) and Aurélie Maspataud (BRGM) for support and photograph facilities during field work, Pauline Cordier (BRGM, Papeete, Tahiti) for logistic support and Virginie Duvat for advices on the field. LFM proposed the topic, conceived the study and served as leader writer, JMB performed analysis and interpretations of electrical resistivity measurements, GLeC collected coral samples and ensured the connection between the contributors, ChI produced U/Th measurements and interpretations, BMG provided the bathymetric profile from the outer reef slope based on his own scuba dives, BS served as a liaison with biologists and geologists, LFM and BMG conceived the illustrations, and BMG produced them. All authors gave input to the paper and approved it. Thanks are given to Yannick Chancerelle and Gilles Siu (Service national d' observation CORAIL, CRIOBE, French Polynesia) for providing quantitative data on coral coverage. This contribution is part of the STORISK research project (N° ANR-15-CE03-0003). Finally, thanks are given to Daniele Spatola (Sapienza University, Roma) and an anonymous reviewer for their constructive comments.

References

Aharon, P., Veeh, H.H., 1984. Isotope studies of insular phosphates explain atoll phosphatization. Nature 308 : 614-617.

Andréfoüet, S., Ardhuin, F., Queffeulou, P., Le Gendre, R., 2012. Island shadow effect and the wave climate of the Western Tuamotu Archipelago (French Polynesia) inferred from altimetry and numerical model data. Marine Pollution Bulletin 65, 415–424.

Bard, E., Hamelin, B., Arnold, M., Montaggioni, L.F., Cabioch, G., Faure, G., Rougerie, F., 1996. Deglacial sea-level record from Tahiti corals and the timing of global meltwater discharge. Nature 382, 241–244.

Bard, E., Hamelin, B., Delanghe-Sabatier, D., 2010. Deglacial Meltwater Pulse 1B and Younger Dryas sea level revisited with boreholes at Tahiti. Science 327, 1235–1237.

Barry, S.J., Cowell, P.J., Woodroffe, C.D., 2007. A morphodynamic model of reef-island de- velopment on atolls. Sedimentary Geology 197, 47–63.

570 Bourrouilh-Le Jan, F.G., Talandier, J., 1985. Sédimentation et fracturation de haute énergie en milieu récifal:
571 tsunamis, ouragans et cyclones et leurs effets sur la sédimentologie et la géomorphologie d'un atoll: motu et hoa,
572 Rangiroa, Tuamotu, Pacifique SE. Marine Geology 67, 263–272.

573 Camoin, G. F., Ebren, Ph., Eisenhauer, A. Bard, E., Faure, G., 2001. A 300 000-yr coral reef record of sea-level
574 changes, Mururoa atoll (Tuamotu Archilago, French Polynesia). Palaeogeography, Palaeoclimatology,
575 Palaeoecology 175, 325–341.

576 Canavesio, R., 2014. Estimer les houles cycloniques à partir d'observations météorologiques limitées: exemple
577 de la submersion d'Anaa en 1906 aux Tuamotu (Polynésie Française). Vertigo 14, doi:10.4000/vertigo.15375

578 Canavesio, R., Pons-Branchu, E., Chancerelle, Y., 2018. Limitations to U/Th dating of reef-platform carbonate
579 boulders produced by high-energy marine inundations in the Tuamotu Archipelago (French Polynesia). Coral
580 Reefs 37, 1139–1155.

581 Carrière, S.D., Chalikakis, K., Sénéchal, G., Danquigny Ch., Emblanch, Ch., 2013. Combining electrical
582 resistivity tomography and ground penetrating radar to study geological structuring of karst unsaturated zone.
583 Journal of Applied Geophysics 94, 31–41.

584 Chen J.H., Edwards R.L., Wasserburg G.J., 1986. ^{238}U, ^{234}U and ^{232}Th in seawater. Earth and Planetary Science
585 Letters 80, 241–251.

586 Chevalier, J.-P., Denizot, M., Mougin, J.L., Plessis, Y., Salvat, B., 1968. Etude géomorphologique et
587 bionomique de l'atoll de Mururoa (Tuamotu). Cahiers du Pacifique 12, 1–144.

588 Clark, P.U., Shakun, J.D., Marcott, S.A., Mix, A.C., Eby, M., Kulp, S., Levermann, A., Milne, G.A., Pfister,
589 P.L., Santer, B.D., Schrag, D.P., 2016. Consequences of twenty-first-century policy for multi-millennial climate
590 and sea-level change. Nature climate change 6, 360–369.

591 Clouard, V., Bonneville, A., 2003. Submarine landslides in Society and Austral Islands, French Polynesia:
592 evolution with the age of edifices. In: Locat, J., Mienert, J., and Boivert, L. (eds). Submarine mass movements
593 and their consequences. Advances in Natural and Technological Hazard Research, vol. 19, Springer, Dordrecht,
594 pp. 335–341.

595 Clouard, V., Bonneville, A., 2004. Submarine landslides in French Polynesia. In: Hekinian, R., Cheminée, J.L.,
596 and Stoffers, P. (eds.), Oceanic Hotspots. Springer, Berlin, pp. 209–238 https://doi.org/10.1007/978-3-642-
597 18782-7_7.

598 Clouard, V., Bonneville, A., Gillot, P.-Y., 2001. A giant landslide on the southern flank of Tahiti Island, French
599 Polynesia. Geophysical Research Letters 28, 2253–2256.

600 Comte J.C., Banton O., Join J.L., Cabioch G., 2010. Evaluation of effective groundwater recharge of freshwater
601 lens in small islands by the combined modeling of geoelectrical data and water heads. Water Resour. Res. 46,
602 W06601. doi:10.1029/2009WR008058

603 Crough, S.T., 1983. Hotspot swells. Annual Reviews of Earth and Planetary Sciences 11, 165–193.

604 Delesalle, B., 1985. Mataiva Atoll, Tuamotu Archipelago. Proceedings of the Fifth International Coral reef
605 Congress, Tahiti 1, 271–321.

606 Dickinson, W.R., 1999. Holocene sea-level record on Funafuti and potential impact of global warming of central
607 Pacific atolls. Quaternary research 51, 123–132.

608 Dickinson, W.R., 2009.Pacific atoll living: how long already and until when. GSA Today19, 4–10.

609 Dullo, W.-Chr, 2005. Coral growth and reef growth: a brief review. Facies 51, 33–48.

610 Dupon, J.-F., 1987. Les atolls et le risque cyclonique. Le cas des Tuamotu. Cahier des Sciences Humaines 23,
611 567–599.

612 Dutton, A., Lambeck, K., 2012. Ice volume and sea level during the last interglacial. Science 337, 216–219.

613 Duvat, V., Volto, N., Pignon-Mussaud, C., Costa, S., Maquaire, O., Davidson, R., 2020. Contrasting atoll island
614 physical robustness advocates for within-atoll relocation, Rangiroa, French Polynesia.

615 East, H.K., Perry, C.T., Kench, P.S., Liang, Y., Gulliver, P., 2018. Coral reef island initiation and development
616 under higher than present sea levels. Geophysical Research Letters 45, 11,265–11,274.

617 Edwards R.L., Chen J.H., Wasserburg G.J., 1987. ^{238}U-^{234}U-^{230}Th-^{232}Th systematics and the precise
618 measurement of time over the past 500,000 years. Earth and Planetary Science Letters 81, 175-192.

619 Etienne, S., 2012. Marine inundation hazards in French 896 Polynesia: geomorphic im- pacts of Tropical
620 Cyclone Oli in February 2010. In: Terry, J.P., and Goff, J. (eds.), Natural Hazards in the Asia-Pacific Region:
621 Recent Advances and Emerging Concepts. Geological Society of London, Special Publication 361, pp. 21–39.

622 Farquharson, C.G., Oldenburg, D.W., 1998. Non-linear inversion using measures of data misfit and model
623 structure. Geophysical Journal International 134, 213–227

624 Faure, G., Laboute, P., 1984. Formations récifales 1: Définitions des unités récifales et distribution des
625 principaux peuplements de scléractiniaires. In: L'atoll de Tikehau (Archipel des Tuamotu, Polynésie française),
626 Premiers Résultats. Notes et Documents Océanographique 22. Office de Recherche Scientifique et Technique
627 d'Outre-Mer, 108–136.

628 Gabrié, C., Salvat, B., 1985. General features of French Polynesian Islands and their coral reefs. Proceedings of
629 the Fifth International Coral Reef Congress, Tahiti 1, 1–15.

630 Gischler, E., Hudson, J.H., 2019. Holocene tropical reef accretion and lagoon sedimentation: a quantitative
631 approach to the influence of sea-level rise, climate and subsidence (Belize, Maldives, French Polynesia). The
632 Depositional Record 5, 515–539.

Hallmann, N., Camoin, G., Eisenhauer, A., Botella, A., Milne, G.A., Vella, C., Samankassou, E., Pothin, V., Dussouillez, P., Fleury, J., Fietzke, J., 2018. Ice volume and climate changes from a 6000 year sea-level record in French Polynesia. Nature Communications 9. https://doi. org/10.1038/s41467-017-02695-7.

Hallmann, N., Camoin, G., Eisenhauer, A., Samankassou, Vella, C., Botella, A., Milne, G.A., Pothin, V., Dussouillez, P., Fleury, G., Fietzke, J., Goepfert, G., 2020. Reef response to sea level and environmental changes in the Central South Pacific over the past 6000 years. Global and Planetaty Change 195, 103357.

Harmelin-Vivien, M.L., 1994. The effects of storms and cyclones on coral reefs: a review. Journal of Coastal Research, Special Issue 12, Coastal Hazards, 211–231.

Harmelin-Vivien, M.L., Laboute, P., 1986. Catastrophic impact of hurricanes on atoll outer reef slopes in the Tuamotu (French Polynesia). Coral Reefs 5, 55–62.

Hubbard, D. K., Dullo, W. Ch., 2016. The Changing Face of Reef Building. In: Hubbard, D. K., Rogers, C. S., Lipps, J. H. and Stanley, G. D. (eds). Coral Reefs at the Crossroads, Coral Reefs of the World, 6. Springer, Dordrecht, pp. 127–153.

Innocent, Ch., Fléhoc, C., Lemeille, F., 2005. U-Th vs. AMS ^{14}C dating of shells from the Achenheim loess (Rhine Graben). Bulletin de la Société Géologique de France 176, 249–255.

IPCC Special Report on the Ocean and Cryosphere in a Changing Climate (Pörtner H.O., .Roberts, D.C., Masson-Delmotte, V., Zhai, P., Tignor, M., Poloczanska, E., Mintenbeck, K., .Alegría, A., Nicolai, M., Okem, A., Petzold, J., Rama, B., Weyer, N.M. (eds.)], 35 pp.

Join J.L., Banton O., Comte J.C., Leze J., Massin F., Nicolini E., 2011. Assessing spatio-temporal patterns of groundwater salinity in small coral islands in the Western Indian Ocean. West Indian Ocean. Journal of Marine Sciences 10, 1–12.

Ito, G., McNutt, M., Gibson, R.L., 1995. Crustal structure of the Tuamotu Plateau, 15°S, and implications for its origin. J. Geophys. Res. 100, 8097–8114.

Kench, P.S., McLean, R.F., Nichol, S.L., 2005. New model of reef-island evolution: Maldives, Indian Ocean. Geology 33, 145–148.

Kench, P.S., Smithers, S.G., McLean, R.F., 2012. Rapid reef island formation and stabil- ity over an emerging reef flat: Bewick Cay, northern Great Barrier Reef, Australia. Geology 40, 347–350.

Kench, P.S., Chan, J., Owen, S.D., McLean, R.F., 2014a. The geomorphology, development and temporal dynamics of Tepuka Island, Funafuti atoll, Tuvalu. Geomorphology 222, 46–58.

Kench, P.S., Owen, S.D., Ford, M.R., 2014b. Evidence for coral island formation during rising sea level in the central Pacific Ocean. Geophysical Research Letters 41, 820–827.

Kench, P.S., Thompson, D., Ford, M.R., Ogawa, H., McLean, R.F. 2015. Coral reef islands defy sea-level rise over the past century: records from a central Pacific atoll. Geology 43, 515–518.

Kopp, R.E., Simmons, F.J., Mitrovica, J.X., Maloof, A.C., Oppenheimer, M., 2009. Probablistic assessment of sea level during the last interglacial stage. Nature 462, 863–867.

Lambeck, K., 1981. Flexure of the ocean lithosphere from island uplift, bathymetry and geoid height observations: the Society Islands. Geophysical Journal of the Royal Astronomical Society 67, 91–114.

Larrue, S., Chiron, Th., 2010. Les îles de Polynésie Française face à l'aléa cyclonique. Vertigo, 10, DOI: 10.4000/vertigo.10558

Lau, A.Y.A., Terry, J.P., Switzer, A.D., Lee, Y., Etienne, S., 2016. Understanding the history of extreme wave events in the Tuamotu Archipelago of French Polynesia from large carbonate boulders on Makemo Atoll, with implications for future threats in the central South Pacific. Marine Geology 380, 174–190.

Loke, M.H., Acworth, I., Dahlin, T. 2003. A comparison of smooth and blocky inversion methods in 2D electrical imaging survey. Exploration Geophyics 34, 182–187.

Marty, J.C., Cazenave, A. 1989. Regional variations in subsidence rate of oceanic plates: a global analysis. Earth and Planetary Science Letters 94, 301–315.

McLean, R.F., Stoddart, D.R., Hopley, D., Polach, H.A., 1978. Sea level change in the Holocene on the northern Great Barrier Reef. Philosophical Transactions of the Royal Society A 291, 167–186.

McNutt, M., Menard, H.W., 1978. Lithospheric flexure and uplifted atolls. Journal of Geophysical Research 83, 1206–1212.

Menard, H.W., 1973. Depth anomalies and the bombing motion of drifting islands. Journal of Geophysical Research 78: 5128-5137.

Millot, R., Guerrot, C., Innocent, Ch., Négrel, P., Sanjuan, B., 2011. Chemical, multi-isotopic (Li-B-Sr-U-H-o) and thermal characterization of Triassic formation waters from the Paris Basin. Chemical Geology 283, 226–241.

Montaggioni, L.F., 1978. Recherches géologiques sur les complexes récifaux de l'archipel des Mascareignes (Océan Indien occidental). Unpublished D.Sc.Thesis, University of Aix-Marseille II, 254 p + annexes.

Montaggioni, L.F., 1985. Makatea Island, Tuamotu Archipelago. Proceedings of the Fifth International Coral Reef Congress, Tahiti 1, 103–158.

Montaggioni, L.F., 1989. Le soulèvement polyphasé d'origine volcano-isostasique: clef de l'évolution post-oligocène des atolls du nord-oust des Tuamotus (Pacifique central). Comptes Rendus de l'Académie des Sciences, Paris, t. 309, Série II, 1591–1598.

Montaggioni, L.F., 2005. History of Indo-Pacific coral reef systems since the last deglaciation: development patterns and controlling factors. Earth Science Reviews 71, 1–75.

Montaggioni L.F., 2011. Conglomerates. In: Hopley, D. (ed) Encyclopedia of Modern Coral Reefs. Encyclopedia of Earth Sciences Series. Springer, Dordrecht. https://doi.org/10.1007/978-90-481-2639-2_201

Montaggioni, L.F., Pirazzoli, P.A., 1984. The significance of exposed coral conglomerates from French Polynesia (Pacific Ocean) as indicators of recent relative sea-level changes. Coral Reefs 3, 29–42.

Montaggioni, L.F., Lauriat-Rage, A., Von Cosel, R., Dolin, L., Le Calvez, Y., Merle, D., Roman, J., Vénec-Peyré, M.-Th., 1985. Depositional environments and paleoecology of an early Miocene atoll-like reef platform (Makatea Island, Central Pacific). Proceedings of the Fifth International Coral Reef Congress, Tahiti 6, 575–580.

Montaggioni, L.F., Camoin, G.F., 1997. Geology of Makatea Island, Tuamotu Archipelago, French Polynesia. In: Vacher, H.L., Quinn, T.M. (eds) Geology and hydrogeology of carbonate islands. Developments in Sedimentology, 54, Elsevier, Amsterdam, pp. 453-473.

Montaggioni, L.F., Salvat, B., Aubanel, A., Eisenhauer, A., Martin-Garin, B. 2018. The mode and timing of windward reef-island accretion in relation with Holocene sea-level change: a case study from Takapoto Atoll, French Polynesia. Geomorphology 318, 320–335.

Montaggioni, L.F., Salvat, B., Aubanel, A., Pons-Branchu, E., Martin-Garin, B., Dapoigny, A., and Goeldner-Gianella, L. 2019 a. New insights into the Holocene development history of a Pacific, low-lying coral reef island: Takapoto Atoll, French Polynesia. Quaternary Science Reviews, 223, 105947.

Montaggioni, L.F., Collin, A., Salvat, B., Martin-Garin, B., Siu, G., Taiarui, M Chancerelle, Y. 2019b. Morphology of fore-reef slopes and terraces, Takapoto Atoll (Tuamotu Archipelago, French Polynesia, central Pacific): the tectonic, sea-level and coral-growth control. Marine Geology 417, 106027.

Murray-Wallace, C.V., Woodroffe, C.D., 2014. Quaternary Sea-level Changes. Cambrige Univ. Press, Cambridge, UK, 484 p.

Obellianne, J.M., 1963. Le gisement de phosphate tricalcique de Makatea (Polynésie Française, Pacifique sud). Sciences de la Terre 9, 5–60.

Paris, R., Ramalho, R.S., Madeira, J., Avila, S., May, S.M., Rixhon, G., Engel, M., Brückner, H., Herzog, M., Schukraft, G., Perez-Torrado, F.J., Rodriguez-Gonzalez A., Carracedo, J.-C., Giachetti, Th., 2013. Mega-tsunami conglomerates and flank collapses of ocean island volcanoes. Marine Geology 395, 168–187.

Parsons, B.E., Sclater, J.G., 1977. An analysis of the variation of ocean floor bathymetry and heat flow with age. Journal of Geophysical Research 82, 803–827.

Perry, C.T., Kench, P.S., Smithers, S.G., Riegl, B., Yamano, H., O'Leary, M.J., 2011. Implications of reef ecosystem change for the stability and maintenance of coral reef islands. Global Change Biology 17, 3679–3696.

Perry et al., 2018. Loss of coral reef growth capacity to track future increases in sea level. Nature doi.org/10.1038/s41586-018-0194-z.

729 Pirazzoli, P.A., Montaggioni, L.F., 1986. Late Holocene sea-level changes in the northwest Tuamotu Islands,
730 French Polynesia. Quaternary Research 25, 350–368.

731 Pirazzoli, P.A., Montaggioni, L.F., 1988. Late Holocene sea-level changes in French Polynesia.
732 Palaeogeography, Palaeoclimatology, Palaeoecology 68, 153–175.

733 Rashid, R., Eisenhauer, A., Stocchi, P., Liebetrau, V., Fietzke, J., Rüggeberg, A., Dullo, W.-Ch., 2014.
734 Constraining mid to late Holocene relative sea-level change in the southern equatorial Pacific Ocean relative to
735 the Society Islands, French Polynesia. Geochemistry, Geophysics, Geosystems 15, 2601–2615.

736 Ricard, M., 1985. Rangiroa Atoll, Tuamotu Archipelago. Proceedings of the Fifth International Coral Reef
737 Congress, Tahiti 1, 161– 209.

738 Richmond, B.M., 1992. Development of atoll islets in the central Pacific. Proceedings of the Seventh
739 International Coral Reef Symposium, Guam 2, 1185–1194.

740 Rougerie, F., Fichez, R., Déjardin, P., 1997. Geomorphology and hydrogeology of selected islands of French
741 Polynesia: Tikehau (Atoll) and Tahiti (Barrier reef). In: Vacher, H.L., Quinn, T.M. (eds), Geology and
742 Hydrology of Carbonate Islands, Developments in Sedimentology 54, Elsevier, Amsterdam, The Netherlands,
743 pp. 475–502.

744 Seaton, W.J., Burbey, Th. J., 2002. Evaluation of two-dimensional resistivity methods in a fractured crystalline-
745 rock terrane. Journal of Applied Geophysics 51, 21–41.

746 Schrott, L., Sass, O., 2008. Application of field geophysics in geomorphology: examples and limitations
747 exemplified by case studies. Geomorphology 93, 55–73.

748 Sladen, A., Hébert, H., Schindelé, F., Reymond, D., 2007. Evaluation of far-field tsunami hazard in French
749 Polynesia based on historical and numerical simulations. Natural Hazards and Earth System Sciences 7, 195–
750 206.

751 Stoddart, D.R., 1969. Reconnaissance geomorphology of Rangiroa Atoll, Tuamotu Archipelago. Atoll Research
752 Bulletin 125, 1–31.

753 Stoddart, D.R., McLean, R.F., Scoffin, T.P., Thom, B.G., Hopley, D., 1978. Evolution of reefs and islands,
754 Northern Great Barrier Reef: synthesis and interpretation. Philosophical Transactions of the Royal Society of
755 London B 284, 149–159.

756 Storlazzi, C., Elias, E.P.L., Berkowitz, P., 2015. Many atolls may be uninhabitable within decades due to climate
757 change. Scientific Reports 5, 14546; doi: 10.1038/srep14546.

758 Storlazzi, C.D., Gingerich, S.B., van Dongeren, A., Cheriton, O.M., Swarzenski, P.W., Quataert, E., Voss, C.I.,
759 Field D.W., Annamalai, H., Piniak G.A., McCall, R., 2018. Most atolls will be uninhabitable by the mid-21st
760 century because of sea-level rise exacerbating wave-driven flooding. Science Advances 4, eaap9741, DOI:
761 10.1126/sciadv.aap9741

762 Talandier, J., Okal, E., 1987. Crustal structure in the Society and Tuamotu Islands, Geophys. J. R. Astron. Soc.
763 88: 499-528.

764 Toomey, M.R., Donnelly, J.P., Woodruff, J.D., 2013. Reconstructing mid-late Holocene cyclone variability in
765 the central Pacific using sedimentary record from Tahaa, French Polynesia. Quaternary Science Reviews 77,
766 181–189.

767 Trichet, J., Fikri, A., 1997. Organic matter in the genesis of high-island atoll peloidal phosphorites: the lagoonal
768 link. Journal of Sedimentary Research 67, 891–897.

769 Werner, A.D., Sharp, H.K., Galvis, S. C., Post, V.E.A., Sinclair, P., 2017. Hydrogeology and management of
770 freshwater lenses on atoll islands: review of current knowledge and research needs. Journal of Hydrology 551,
771 819–844.

772 Woodroffe, C.D., 2005. Late Quaternary sea-level highstands in the central and eastern Indian Ocean: a review.
773 Global and Planetary Change 49, 121–138.

774 Woodroffe, C.D., McLean, R.F., Smithers, S.G., Lawson, E.M., 1999. Atoll reef-island formation and response
775 to sea-level change: West Island, Cocos (Keeling) Islands. Marine Geology 160, 85–104.

776 Woodroffe, C.D., Morrison, R.J., 2001. Reef-island accretion and soil development, Makin Island, Kiribati,
777 Central Pacific. Catena 44, 245–261.

778 Woodroffe, C.D., Samosorn, B., Hua, Q., Hart, D.E., 2007. Incremental accretion of a sandy reef island over the
779 past 3000 years indicated by component-specific radiocarbon dating. Geophysical Research Letters 34, L03602,
780 doi:10.1029/2006GL028875

781 Woodroffe, C.D., Biribo, N., 2011. Atolls. In: Hopley, D. (ed) Encyclopedia of Modern Coral Reefs.
782 Encyclopedia of Earth Sciences Series. Springer, Dordrecht, pp.51–71.

783 Yamano, H., Cabioch, G., Chevillon, C., Join, J.L., 2014. Late Holocene sea-level change and reef-island
784 evolution in New Caledonia. Geomorphology 222, 39–45.

785 Yasukochi, T., Kayanne, H., Yamaguchi, T., Yamano, H., 2014. Sedimentary facies and Holocene depositional
786 processes of Laura Island, Majuro Atoll. Geomorphology 222, 59–67.

787 Youssef, A.M., El-Kaliouby, H., Zabramawi, Y.A., 2012. Sinkhole detection using electrical resistivity
788 tomography in Saudi Arabia. Journal of Geophysics and Engineering 9, 655–663.

789 Table 1. Uranium and thorium concentrations in coral samples from the north-eastern rim-
790 island, Rangiroa Atoll. Are given successively, laboratory sample codes, uranium and thorium
791 contents, isotopic composition with statistical errors reported as 2 phi and non-corrected and
792 corrected ages. Total blanks were 18 pg for U and 82 pg for Th.

Table 2. Attempt at interpretation of resistivity data in terms of geological and hydrological features, north-eastern rim-island, Rangiroa Atoll.

Figure 1. A: Location map of the northwestern Tuamotu Atolls in French Polynesia (central south Pacific). B: Map of Rangiroa Atoll showing location of the studied northern areas. C: Aerial view of the studied northern areas at Rangiroa showing location of the two well sites – Well 1 and Well 2 – of U/Th dated Sample Défense and of two electrical resistivity profiles – P1 and P3.

Figure 2. Bathymetric profile along the forereef slope in front of Taputa, northeast of Rangiroa, showing the successive geomorphic feature from surface to –60 m depth.

Figure 3. General view of exposed, about 3 m-high, dolomitized remnants of Miocene limestone pinnacles (*feo*) expected to be Miocene in age. These are peaking through the outer reef-flat flat zone; in the background of the picture, on the left, appear two vegetated atoll islets and, on the right, the wave-breaking, reef-crest zone. Photograph courtesy by Philippe Bacchet.

Figure 4. Internal view of Well 1 and Well 2 showing the walls from which coral clasts were collected, northern Rangiroa. Photographs by Aurélie Maspataud.

Figure 5. Sections of Well 1 (2.0–2.30 m deep) and Well 2 (1.5–1.6 m deep) northern Rangiroa, showing location of U/Th–dated coral clasts collected along the internal walls. The two logs shown for each well relate to the opposite well sides of each site.

Figure 6. Uranium isotope characteristics of dated coral samples. A: Comparison between uranium contents and the average value of living corals (blue line). Analytical uncertainties are smaller than the sizes of the symbols. B: Uranium activity ratios for the analyzed coral samples. The blue line represents the seawater value, the dotted lines relate to uncertainties on the average value.

Figure 7. Electrical resistivity tomography (ERT) profiles, close to Avatoru Village, northern Rangiroa (see Fig. 1C for location of the two profiles). (A) Interpretated N–S Profile P1. B: Interpretated N–S Profile P3. C: Conceptual geological model of the internal structure of the uppermost carbonate pile based on both interpreted ERT profiles. FWL = Fresh Water Lens.

Figure 8. Comparing periods of coral-clast supply for rim-island accretion between Rangiroa and Takapoto Atolls, relative to the course of sea level over the last 12,000 years. The relative sea-level curve is based on data from Pirazzoli and Montaggioni (1988), Bard et al. (1996, 2010) and Hallmann et al. (2018, 2020).

Figure 9. Plotted U/Th ages of the five coral clasts *versus* elevation – relative to present mean sea level – collected in Well 1 and Well 2 (northern Rangiroa) compared with the U/Th age-elevation cluster of the 79 coral samples collected from the eight holes excavated through southeastern and south-western island sites at Takapoto Atoll (Montaggioni et al., 2018, 2019a). Note that among the 80 dated coral samples at Takapoto, only one sample (dated at 7,705 ± 120 cal. yr) from the base of an excavation site is outside of the cluster.

Figure 10. Northern Rangiroa Atoll: conceptual model of rim-island accretion from 8,000 to 3,500 cal. yr. A: 8,000 cal. yr: the top of the Miocene-Pleistocene carbonate pile culminated at an elevation of about 15 m above sea level and was clast-supplied by extreme wave-surge events. B: 6,000 cal. yr: sea level reached and outpassed its present position, thus flooded the carbonate pile. The Holocene unit develops in the form of an about 5 m-thick bed. Coral-clast deposition resulted in the formation of depocentres mainly composed of skeletal sands and gravels. C: 3,000 cal.yr: sea level was falling down. The rim-island initiation phase was achieved and islets continued to accrete laterally and vertically.

Figure 11. Takapoto Atoll: conceptual model of rim-island development from 8,000 to 1,500 cal. yr – adapted from Montaggioni et al., 2018, 2019a. A: 8,000 cal. yr: the top of the carbonate pile – late Pleistocene in age – culminated at an approximate elevation of 9–10 m. B: 6,000 cal. yr: during the sea-level rise, from 8,000 to 6,000 cal. yr, the available accommodation space thus created was partly infilled by mid Holocene coral-reef growth. C: 2,500–1,500 cal. yr: from 6,000 to 5,000 cal. yr, during the final course of the rising sea level, the remaining accommodation space was totally infilled by late Holocene coral growth. From 2,500 cal. yr, coral clasts derived from the adjacent forereef zones were deposited onto the reef-flat surface thus created, resulting in the formation of indurated conglomerates and then unconsolidated gravelly to sandy rim-islets. The 2,500–1,500 cal. yr interval relates to the phase of rim-island initiation.

Figure 12. Conceptual mapping of the northern areas at Rangiroa atoll and of the southeastern area at Takapoto atoll, showing successive rim-island accretion phases. Isochrons delineate

852 the changing aerial extent of islets through time. A: Rangiroa: island accretion from 6,000 cal.
853 yr to present. The development of initial depocentres occurred within the 6,000–3,000 cal. yr
854 time-lines. From about 3,000 cal. yr to present, the islets accreted laterally to vertically to
855 result in the modern island morphology. B: Cross section along the X–Y axis in Figure 12A.
856 C: Takapoto: adapted from Figure 12 in Montaggioni et al. (2019a). This shows the timing of
857 the rim-island development at Takapoto.

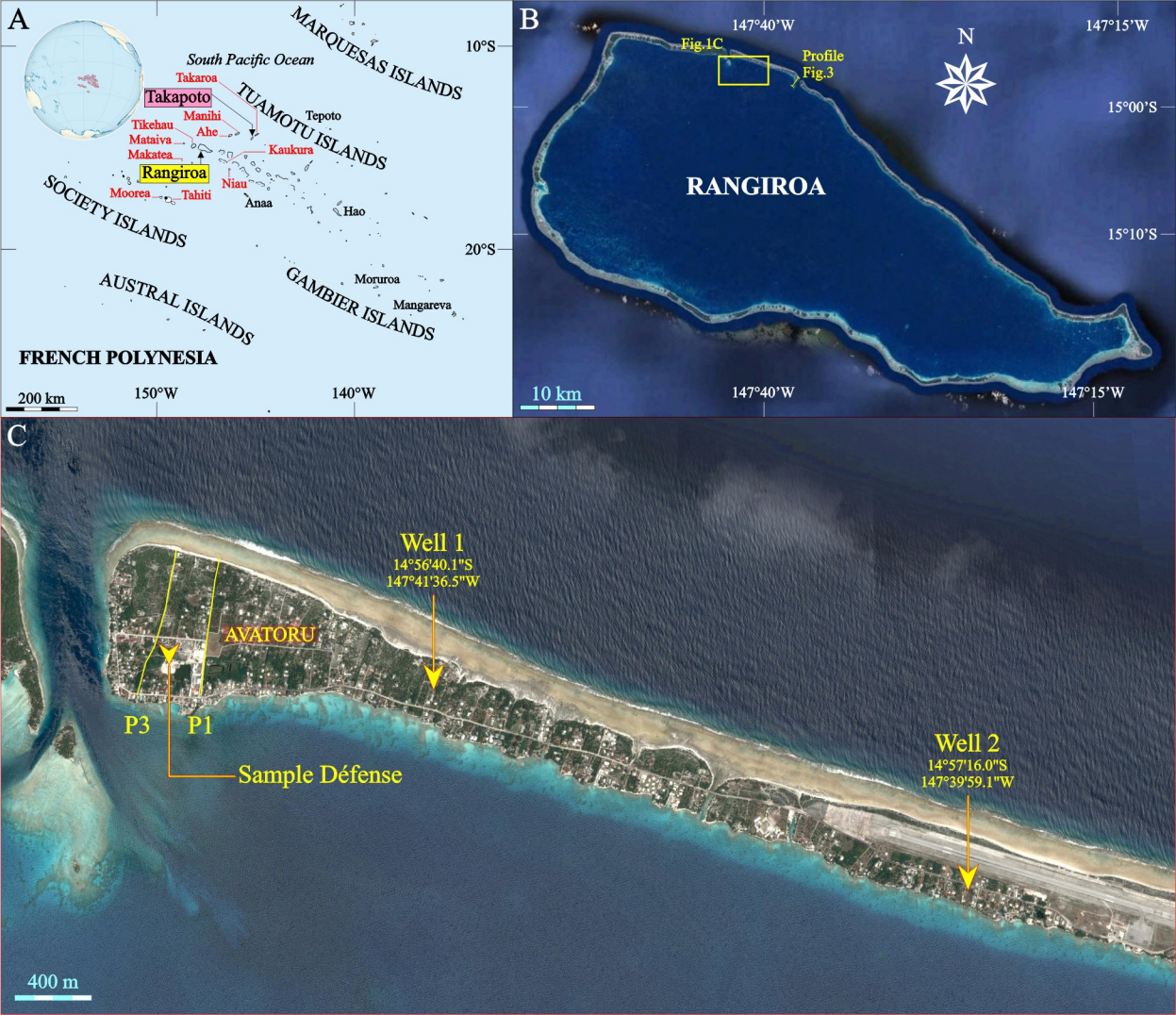
A
South Pacific Ocean
MARQUESAS ISLANDS
TUAMOTU ISLANDS
SOCIETY ISLANDS
AUSTRAL ISLANDS
GAMBIER ISLANDS
FRENCH POLYNESIA
Takaroa
Takapoto
Manihi
Tikehau
Ahe
Mataiva
Makatea
Kaukura
Rangiroa
Niau
Moorea
Tahiti
Anaa
Tepoto
Hao
Moruroa
Mangareva
10°S
20°S
150°W
140°W
200 km
B
147°40'W
147°15'W
Fig.1C
Profile
Fig.3
N
15°00'S
15°10'S
RANGIROA
10 km
C
Well 1
14°56'40.1"S
147°41'36.5"W
AVATORU
P3
P1
Sample Défense
Well 2
14°57'16.0"S
147°39'59.1"W
400 m

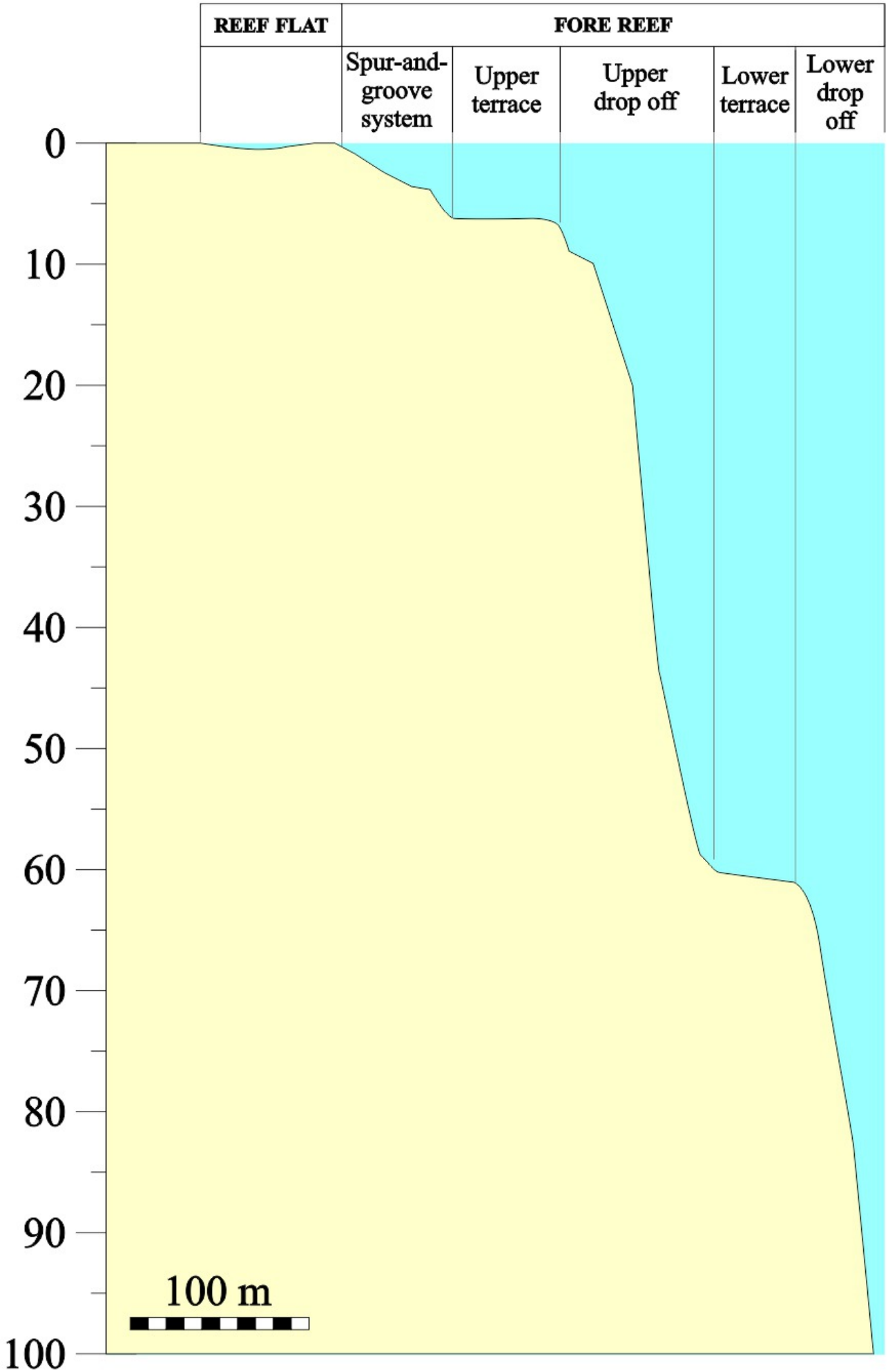
REEF FLAT
FORE REEF
Spur-and-groove system
Upper terrace
Upper drop off
Lower terrace
Lower drop off
0
10
20
30
40
50
60
70
80
90
100
100 m


A


B

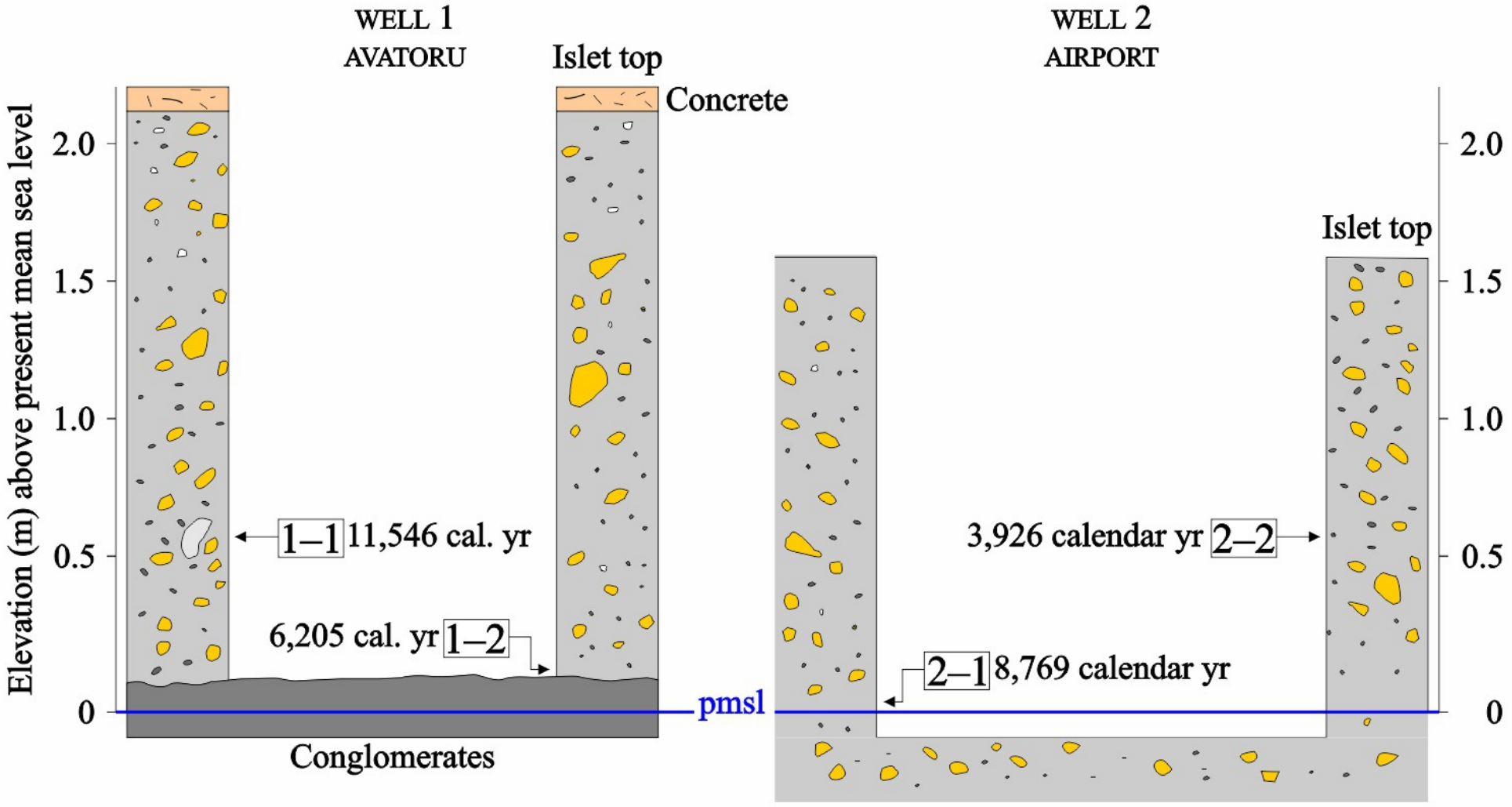
WELL 1
AVATORU
Islet top
Concrete
WELL 2
AIRPORT
Islet top
Elevation (m) above present mean sea level
2.0
1.5
1.0
0.5
0
1–1 11,546 cal. yr
6,205 cal. yr 1–2
3,926 calendar yr 2–2
2–1 8,769 calendar yr
pmsl
Conglomerates

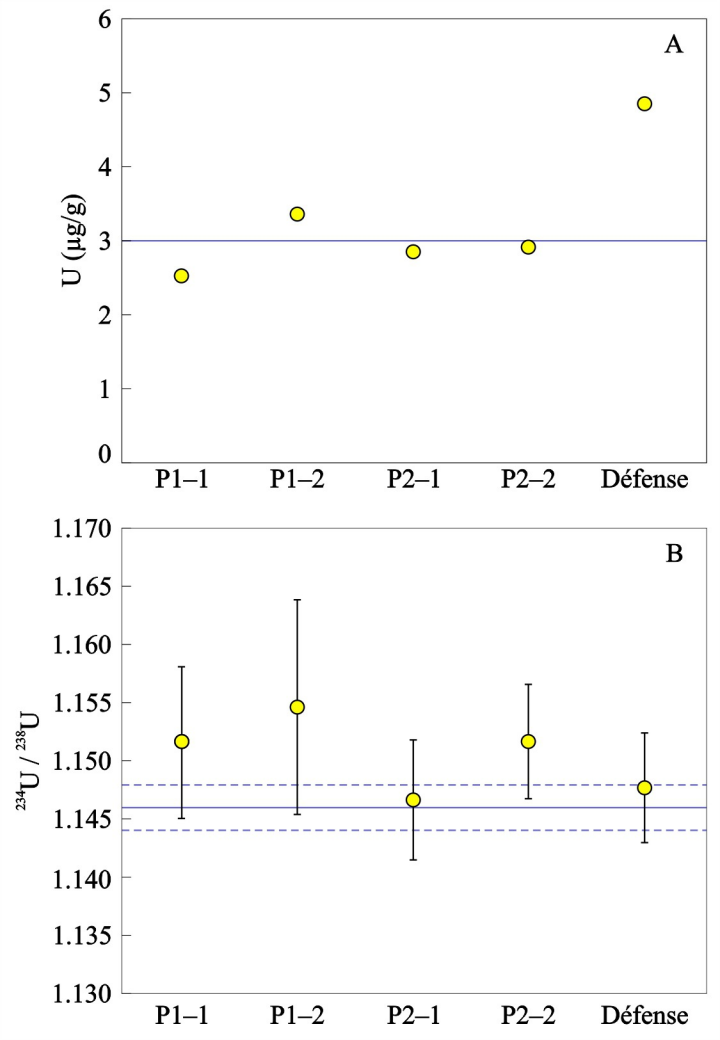
A
U (µg/g)
6
5
4
3
2
1
0
P1–1
P1–2
P2–1
P2–2
Défense
B
234U / 238U
1.170
1.165
1.160
1.155
1.150
1.145
1.140
1.135
1.130
P1–1
P1–2
P2–1
P2–2
Défense

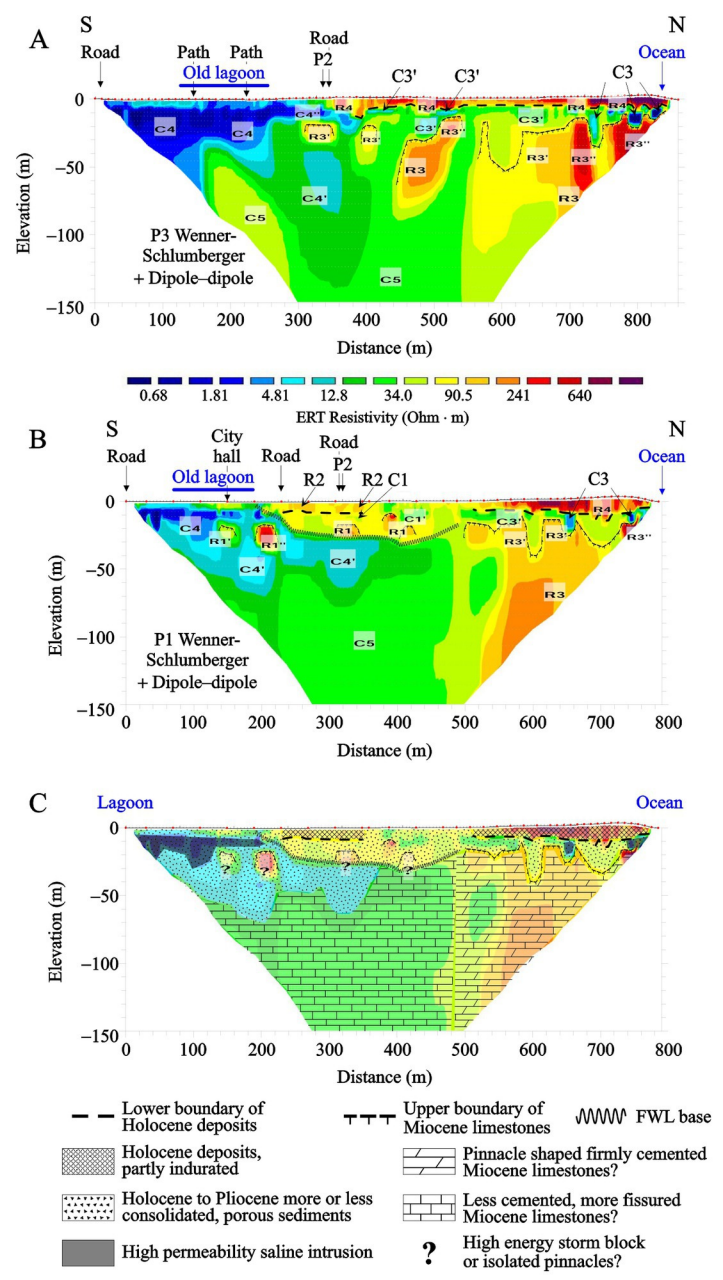
A
S
N
Road
Path
Path
Old lagoon
Road
P2
C3'
C3'
C3
Ocean
Elevation (m)
Distance (m)
P3 Wenner-
Schlumberger
+ Dipole–dipole
0.68
1.81
4.81
12.8
34.0
90.5
241
640
ERT Resistivity (Ohm · m)
B
S
N
Road
City
hall
Road
Road
P2
Old lagoon
R2
R2 C1
C3
Ocean
Elevation (m)
Distance (m)
P1 Wenner-
Schlumberger
+ Dipole–dipole
C
Lagoon
Ocean
Elevation (m)
Distance (m)
Lower boundary of
Holocene deposits
Upper boundary of
Miocene limestones
FWL base
Holocene deposits,
partly indurated
Pinnacle shaped firmly cemented
Miocene limestones?
Holocene to Pliocene more or less
consolidated, porous sediments
Less cemented, more fissured
Miocene limestones?
High permeability saline intrusion
?
High energy storm block
or isolated pinnacles?

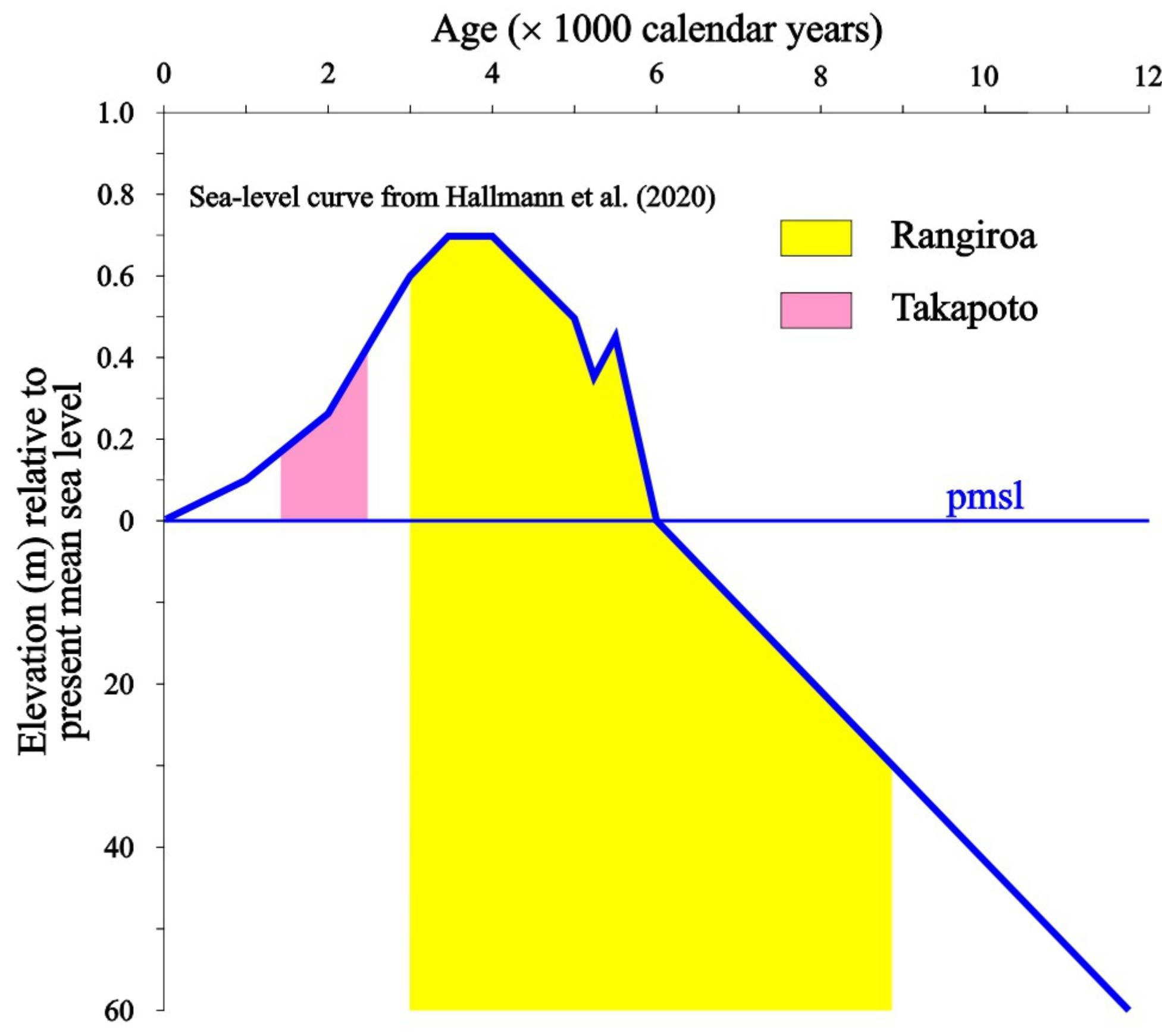
Age (× 1000 calendar years)
0
2
4
6
8
10
12
1.0
0.8
0.6
0.4
0.2
0
20
40
60
Elevation (m) relative to present mean sea level
Sea-level curve from Hallmann et al. (2020)
Rangiroa
Takapoto
pmsl

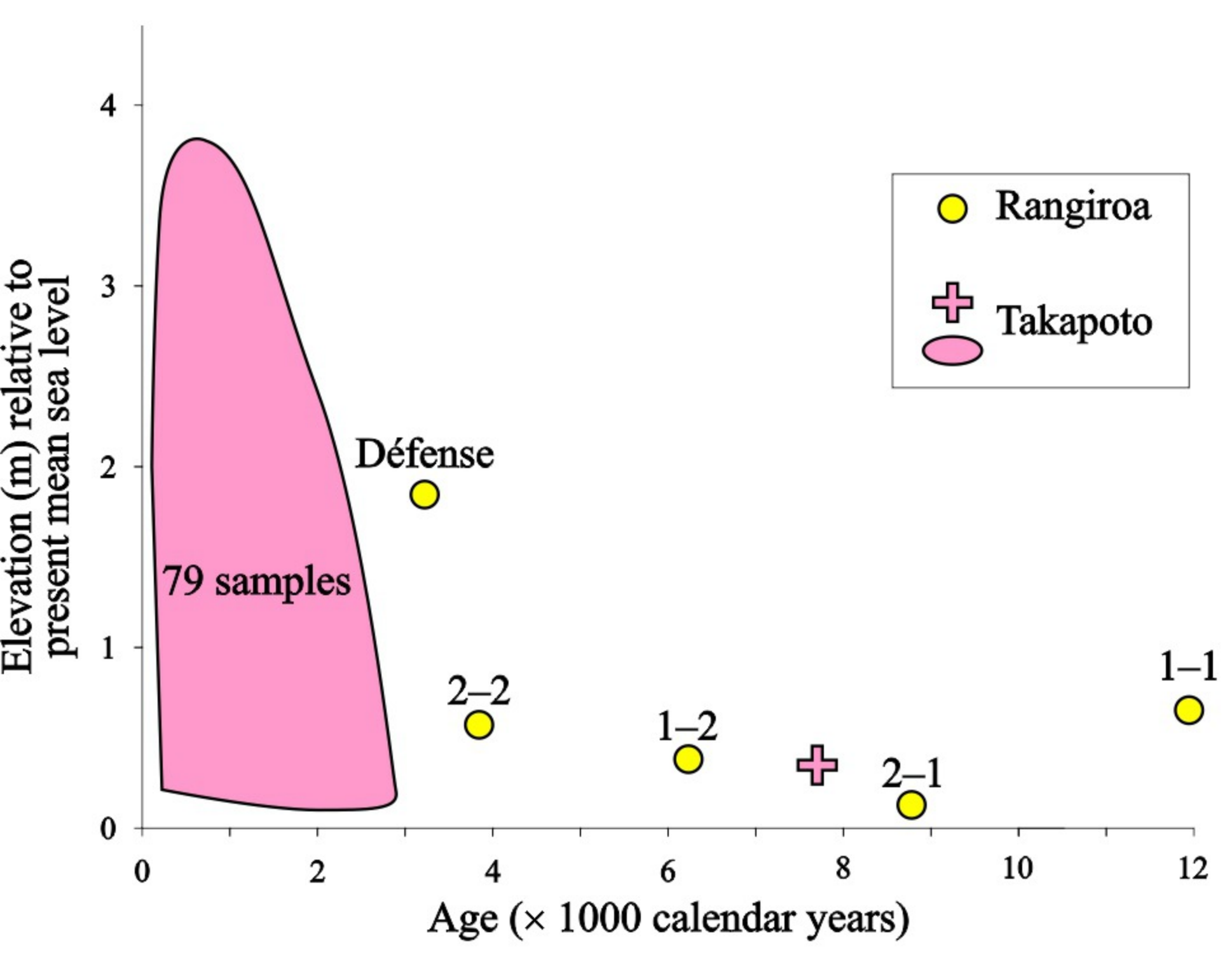
Elevation (m) relative to present mean sea level
4
3
2
1
0
0
2
4
6
8
10
12
Age (× 1000 calendar years)
Rangiroa
Takapoto
Défense
79 samples
2–2
1–2
2–1
1–1

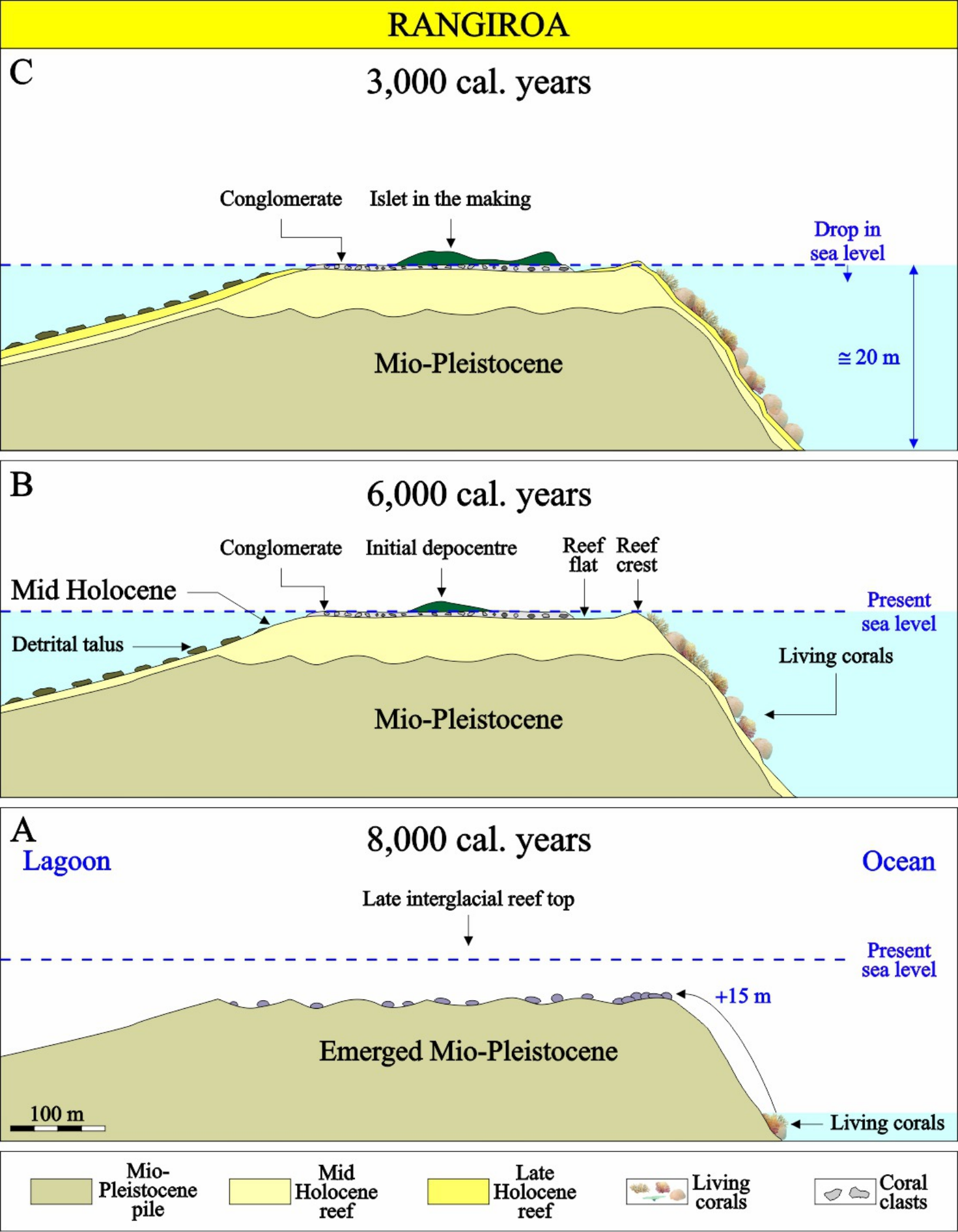
RANGIROA
C
3,000 cal. years
Conglomerate
Islet in the making
Drop in sea level
≅ 20 m
Mio-Pleistocene
B
6,000 cal. years
Conglomerate
Initial depocentre
Reef flat
Reef crest
Mid Holocene
Present sea level
Detrital talus
Living corals
Mio-Pleistocene
A
8,000 cal. years
Lagoon
Ocean
Late interglacial reef top
Present sea level
+15 m
Emerged Mio-Pleistocene
100 m
Living corals
Mio-Pleistocene pile
Mid Holocene reef
Late Holocene reef
Living corals
Coral clasts

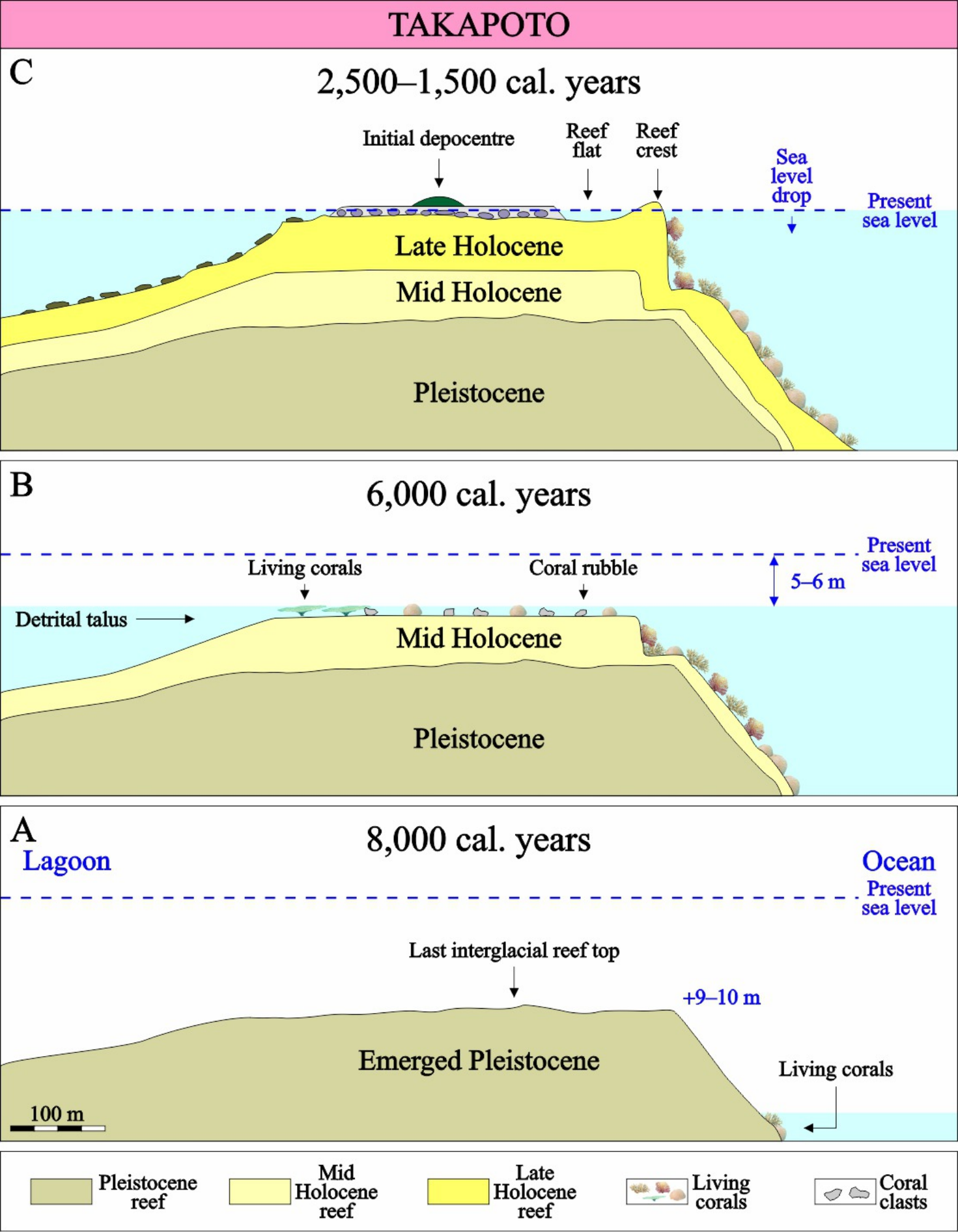
TAKAPOTO
C
2,500–1,500 cal. years
Initial depocentre
Reef flat
Reef crest
Sea level drop
Present sea level
Late Holocene
Mid Holocene
Pleistocene
B
6,000 cal. years
Present sea level
Living corals
Coral rubble
5–6 m
Detrital talus
Mid Holocene
Pleistocene
A
8,000 cal. years
Lagoon
Ocean
Present sea level
Last interglacial reef top
+9–10 m
Emerged Pleistocene
Living corals
100 m
Pleistocene reef
Mid Holocene reef
Late Holocene reef
Living corals
Coral clasts

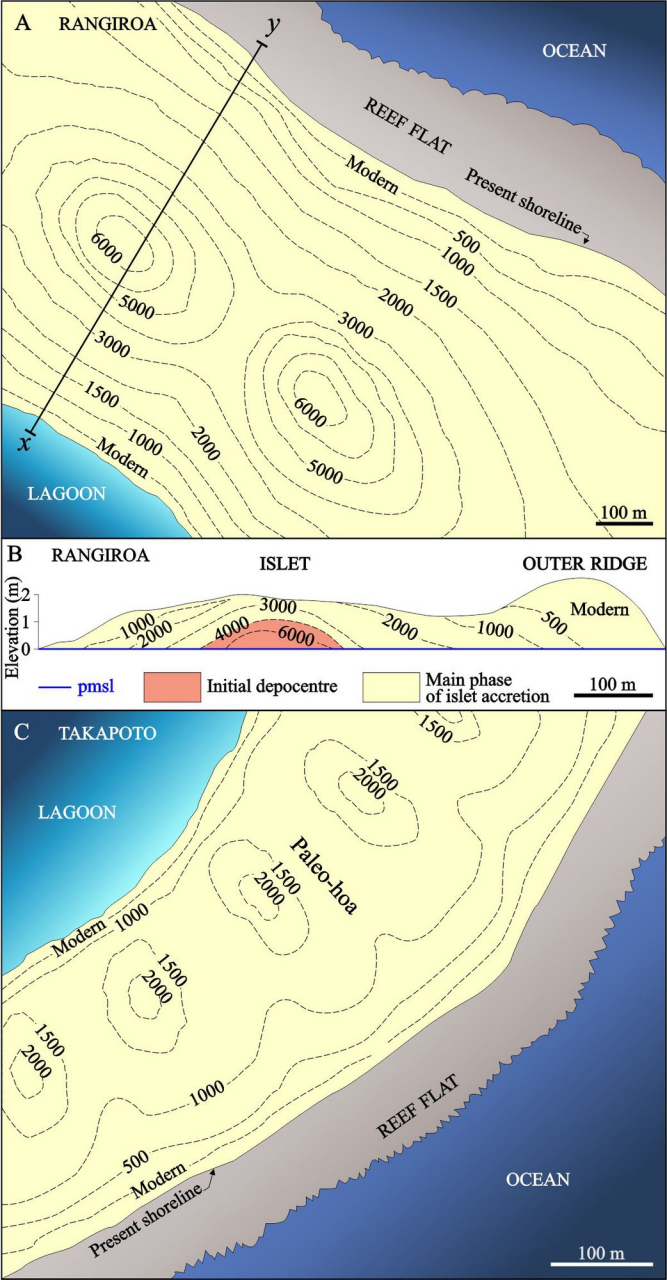
A
RANGIROA
y
x
OCEAN
REEF FLAT
Present shoreline
Modern
500
1000
1500
2000
3000
5000
6000
LAGOON
100 m
B
RANGIROA
ISLET
OUTER RIDGE
Elevation (m)
2
1
0
Modern
pmsl
Initial depocentre
Main phase of islet accretion
100 m
C
TAKAPOTO
LAGOON
Paleo-hoa
Modern
REEF FLAT
OCEAN
Present shoreline
100 m

Resistivity units		**Possible geological and hydrological features**	**Remarks**
R3, R3', R3"	Resistive units at the seaward side of the atoll-rim pile ($90 < \rho < 500\ \Omega \cdot m$) with upward columnar extensions.	Miocene cemented and karstified limestone basement, possibly dolomitized.	
R4	Resistive ($90 < \rho < 700\ \Omega \cdot m$) cover at the seaward side of the atoll-rim pile.	Postglacial to Holocene deposits – sand-rubble sheets, conglomerate platforms, isolated megaclasts (?).	Because of the large (10 m) electrode spacing, possible intercalated fresh water lens may be not observed.
R1, R2	Shallow (R2) or deeper (R1) resistive ($90< \rho < 250\ \Omega \cdot m$) cover in the central part of the atoll-rim pile	More or less consolidated sediments bathed by fresh to saline water. With C1, C1' these zones constitute the fresh water lens.	Deeper resistive units (R1) may also correspond to the top of karstified Miocene limestones. Lack of freshwater lens in P3 tomography is explained by its proximity to the pass which favours saline intrusion.
C4, (C4', C4")	Conductive ($0.3 < \rho < 5\ \Omega \cdot m$) cover (C4) at the lagoon side of the atoll-rim pile; less conductive ($5 < \rho < 15\ \Omega \cdot m$) extension (C4', C4") intruding the atoll-rim subsurface.	Large saline intrusion in more or less hydraulically conductive sediments.	C4 may refer to porous, Holocene material. C4' and C4" may refer to large karstic zones within the Miocene basement infilled with porous phosphatic deposits of Pliocene (?) age.
C3, C3'	More (C3 $0.3 < \rho <10\ \Omega \cdot m$) or less intense (C3', $10 < \rho < 60\ \Omega \cdot m$) isolated conductive anomaly.	Isolated saline intrusion, intercalated, porous, weakly consolidated deposits invaded by saline water.	Karstic galleries running into Miocene limestones may be filled with saline water and/or hydraulically conductive sediments, electrically conductive phosphatic deposits of Pliocene (?) age.
C1, C1'	Intercalated conductive layer ($20 < \rho < 60\ \Omega \cdot m$)	Intercalated freshwater and/or more or less salty (C1') aquifer	
C5	Intermediate resistivity basement ($20 < \rho < 60\ \Omega \cdot m$)	Possibly fissures/fractures in Miocene limestone basement.	The reason why internal and external atoll-island substratum presents contrasted resistivity remains a question: differential nature or state of sediments: rubble *versus* sand (?) cementation (?) dolomitization (?)